

## RESEARCH ARTICLE

# Isotopic composition of sinking particles: Oil effects, recovery and baselines in the Gulf of Mexico, 2010–2015

Jeffrey P. Chanton\*, Sarah L.C. Giering<sup>†,‡</sup>, Samantha H. Bosman\*, Kelsey L. Rogers\*, Julia Sweet<sup>†</sup>, Vernon L. Asper<sup>§</sup>, Arne R. Diercks<sup>§</sup> and Uta Passow<sup>†</sup>

The extensive release of oil during the 2010 Deepwater Horizon spill in the northern Gulf of Mexico perturbed the pelagic ecosystem and associated sinking material. To gauge the recovery and post-spill baseline sources, we measured  $\Delta^{14}\text{C}$ ,  $\delta^{13}\text{C}$  and  $\delta^{34}\text{S}$  of sinking particles near the spill site and at a reference site and natural seep site. Particulates were collected August 2010–April 2016 in sediment traps moored at sites with depths of 1160–1660 m. Near the spill site, changes in  $\Delta^{14}\text{C}$  indicated a 3-year recovery period, while  $\delta^{34}\text{S}$  indicated 1–2 years, which agreed with estimates of 1–2 years based on hydrocarbon composition. Under post-spill baseline conditions, carbon inputs to sinking particulates in the northern Gulf were dominated by surface marine production (80–85%) and riverine inputs (15–20%). Near the spill site,  $\Delta^{14}\text{C}$  values were depleted in October 2010 ( $-140$  to  $-80\text{‰}$ ), increasing systematically by  $0.07 \pm 0.02\text{‰ day}^{-1}$  until July 2013 when values reached  $-3.2 \pm 31.0\text{‰}$ . This  $\Delta^{14}\text{C}$  baseline was similar to particulates at the reference site ( $3.8 \pm 31.1\text{‰}$ ). At both sites,  $\delta^{13}\text{C}$  values stayed constant throughout the study period ( $-21.9 \pm 0.5\text{‰}$  and  $-21.9 \pm 0.9\text{‰}$ , respectively).  $\delta^{34}\text{S}$  near the spill site was depleted ( $7.4 \pm 3.1\text{‰}$ ) during October 2010–September 2011, but enriched ( $16.9 \pm 2.0\text{‰}$ ) and similar to the reference site ( $16.2 \pm 3.1\text{‰}$ ) during November 2012–April 2015. At the seep site,  $\Delta^{14}\text{C}$  values were  $-21.7 \pm 45.7\text{‰}$  except during August 2012–January 2013 when a significant  $\Delta^{14}\text{C}$  depletion of  $-109.0 \pm 29.1\text{‰}$  was observed. We interpret this depletion period, also observed in  $\delta^{13}\text{C}$  data, as caused by the incorporation of naturally seeped oil into sinking particles. Determination of post-spill baselines for these isotopic signatures allows for evaluation of anthropogenic inputs in future.

**Keywords:** Deep Water Horizon Oil Spill; radiocarbon; isotopes; Gulf of Mexico; sinking particulates; sediment trap

## 1. Introduction

The Deepwater Horizon (DWH) oil spill in the northern Gulf of Mexico was the largest accidental discharge of fossil hydrocarbon in history. The spill started on 20 April 2010 and continued until 15 July 2010. The DWH spill was extraordinary in its depth of release and its volume, some 4.9 million barrels, not including methane, and the large quantity of dispersants that was applied. Also unprecedented was the scientific attention focused on the accident and the response of the ecosystem. One of the more unexpected results for response planners was the extensive sedimentation of oil-associated marine snow to

the deep seafloor, making up as much as 14% (Daly et al., 2016; Passow and Hetland, 2016; Passow and Ziervogel, 2016) of the quantity of oil released. The sedimentation of oil to the deep seafloor is thought to have been mediated, at least in part, by the so-called MOSSFA process (marine oil snow sedimentation and flocculent accumulation; Daly et al., 2016).

The MOSSFA process is driven by aggregation of phytoplankton and the incorporation of oil (Passow et al., 2012; Passow and Ziervogel, 2016). This process is linked to the production of transparent exopolymeric particles (TEP), which are sugar-based gluey binders that often form the matrix of marine snow and promote aggregation. Marine snow coagulates with oil to form ‘marine oil snow’ that can transport otherwise buoyant oil to depth. This process is considered distinct from sinking oil-mineral aggregates (OMAs), where oil itself is ballasted with mineral particles, thus increasing the density and allowing oiled material to sink (Muschenheim and Lee, 2002). Sinking velocity of the marine oil snow collected during the DWH spill

\* Florida State University, Tallahassee, Florida, US

<sup>†</sup> University of California, Santa Barbara, California, US

<sup>‡</sup> National Oceanography Centre, Southampton, UK

<sup>§</sup> University of Southern Mississippi, Stennis Space Center, Mississippi, US

Corresponding author: Jeffrey P. Chanton ([jchanton@fsu.edu](mailto:jchanton@fsu.edu))

varied from 68 to 553 m d<sup>-1</sup>, a range similar to marine snow without oil (Diercks and Asper, 1997; Passow et al., 2012). During the DWH spill, marine oil snow may also have been produced at depth from the 1000-m deep subsurface plume which emanated from the busted well head and moved to the southwest (Camilli et al., 2010; Diercks et al., 2010). Sinking marine snow may have scavenged oil while sinking through the plume or through enhanced microbial activity in response to the released oil (Valentine et al., 2014), serving as a cleansing agent for the water column (Yan et al., 2016).

During the DWH event, substantial amounts of oil were transported to the seafloor by MOSSFA events (Brooks et al., 2015; Schwing et al., 2017), though estimates of the absolute amount vary considerably. Valentine et al. (2014) used hopane as a tracer and estimated that 4–31% of the deep sea plume went to the seafloor, or 2–14% of the total oil assuming a total release of 4.1 to 4.6 million barrels (Lehr et al., 2010; Joye et al., 2011; Griffiths, 2012; McNutt et al., 2012). Stout et al. (2017) also used hopane and estimated that 7–8% of 3.2 million barrels spilled were deposited on the deep water seafloor, which would translate to 5–6% if the larger volume of oil discharge had been used. Chanton et al. (2015) employed radiocarbon and estimated that 0.5–9% of the oil went to the seafloor, with a best estimate of 3–5% of 4.1–4.6 million barrels released. Romero et al. (2017), using a number of hydrocarbon indicators, estimated  $2 \pm 0.5\%$  of the spilled oil was deposited in the deep gulf. These estimates may be lower limits of oil deposition for a variety of reasons. They likely indicate net deposition, not total deposition as they do not consider resuspension, mobilization and degradation of oil. In addition, the areal extent of the areas that were considered may have been too limited (Stout and German, 2015; Passow and Hetland, 2016; Passow and Ziervogel, 2016).

The lack of knowledge regarding pre-oil conditions in the Gulf impaired assessment of the impacts of the DWH spill. To allow better ecological assessments following any future spills, knowing the Gulf's baseline conditions is essential, as discussed by Giering et al. (2018). A robust method for determining the baseline is tracing the isotopic signature of organic matter inputs into the Gulf ecosystem.

The term “petrocarbon” broadly describes crude oil or the products of transformed crude oil such as oxygenated products (e.g., Ruddy et al., 2014). Petrocarbon also includes oil- or methane-derived organic material incorporated into bacteria (Cherrier et al., 2014) or into the food web (Chanton et al., 2012; Wilson et al., 2016). The term is distinct from the term “petrogenic”, which includes fossil (aged, isotopically depleted) elements released from rocks. The isotopic signature of an element (i.e., the ratio of different isotopes of, e.g., carbon) can be used to track the element's origin and can reveal the presence of petrocarbon even when the original oil or methane has been transformed and lost its unique chemical structure. The chemistry of a petroleum-based molecule can be altered, for example, by oxygenation (Ruddy et al., 2014) which can affect the molecule's polarity, solubility and reactivity, yet the molecule will still carry the original isotopic signature.

In the Gulf of Mexico, petrocarbon may be mixed with recently photosynthesized organic matter and/or river-delivered terrestrial organic matter. Each of these endmembers has a unique isotopic signature. In such environments where particle fluxes originate from different sources, the combination of different isotopic signatures can thus be used to determine the source contributions using endmember mixing analysis.

There are three carbon isotopes that occur naturally: the stable <sup>12</sup>C which makes up ~99% of the carbon, and the two tracers <sup>13</sup>C and <sup>14</sup>C. Of the two tracers, radiocarbon <sup>14</sup>C is more sensitive for the determination of the presence of petrocarbon released into the environment (Bosman et al., 2017). In the Gulf of Mexico, the  $\Delta^{14}\text{C}$  values of the three endmembers are ~40‰ for recently photosynthesized marine carbon (Chanton et al., 2012), -86 to -223‰ for river-delivered terrestrial carbon (Chanton et al., 2015; Rosenheim et al., 2013), and -1000‰ for petrocarbon. In terms of the natural radiocarbon abundance <sup>14</sup>C, oil spills have been described as “inverse tracer experiments” (Reddy et al., 2002; White et al., 2005, 2008). The DWH spill added radiocarbon-free fossil carbon to a surficial ecosystem dominated by modern photosynthetic production. Unfortunately, the balance between old and modern carbon in the differing carbon pools of the Gulf of Mexico was poorly quantified prior to the oil spill (Rosenheim et al., 2016).

The scale of variation in the stable isotopic composition ( $\delta^{13}\text{C}$ ) in the Gulf of Mexico is less than that for  $\Delta^{14}\text{C}$ , about 40‰ (compared to about 1040‰); i.e., from -20 to -22‰ for marine primary production and -23.3 to -26.0‰ for riverine material (Chanton et al., 2015; Rosenheim et al., 2013) to -27‰ for DWH oil (Graham et al., 2010) and between -57 and -61‰ for DWH methane (Valentine et al., 2010; Crespo-Medina et al., 2014). Thus,  $\delta^{13}\text{C}$  is particularly useful for distinguishing methane from petroleum inputs (Cherrier et al., 2014).

Sulfur isotopes,  $\delta^{34}\text{S}$ , can be used in a similar fashion to track organic matter sources. Marine sulfate, the primary form of sulfur in oxic surface waters, has a  $\delta^{34}\text{S}$  value of about 20‰ (Rees et al., 1978). During primary production, sulfur is incorporated into biomass by the assimilatory sulfate reduction process which does not significantly fractionate sulfur isotopes; thus marine primary production has a  $\delta^{34}\text{S}$  value close to 20‰. Terrestrial/riverine sulfur is derived from continental weathering and has a value near 0‰ (Chanton and Lewis, 2002), while petrocarbon may be influenced by sulfide produced during dissimilatory sulfate reduction and have a negative  $\delta^{34}\text{S}$  signature ( $\delta^{34}\text{S} < 0\text{‰}$ ).

This study focused on temporal and spatial variation in the isotopic composition of particulate organic matter (POM) sinking through the water column to the seafloor over the period of time following the DWH oil spill, 2010 to 2016, and had three objectives. The first objective was to test the hypothesis that tracking the temporal trend in the isotopic composition of sinking POM at a site heavily impacted by the oil spill would allow us to determine the recovery time of the system at least in terms of the quantity measured. The second objective was to determine

the baseline isotopic values of sinking particles in the Gulf and the relative importance of the inputs that contribute organic matter to those particles. The third objective was to test the hypothesis that MOSSFA events can occur naturally, at sites dominated by high rates of seafloor seepage of oil and gas. Recently, upwelling caused by high seepage rates has been documented as promoting localized nutrient entrainment and enhanced primary production (D'souza et al., 2016). In addition, these upwardly entrained fluids carry oil, gas, particulates and petrocarbon-rich bacteria from the seep community into the surface waters (Solomon et al., 2009). This petrocarbon, stemming from natural seeps, could be incorporated into sinking marine snow, or be incorporated into food-webs and sink as biological detrital snow, e.g., fecal pellets or biomass. We hypothesized that such natural MOSSFA events might occur regularly and could be captured in the sediment trap positioned near a large natural seep.

## 2. Methods

### 2.1. Deployment sites and sample collection

We collected sedimented material (sinking POM) between 2010 and 2016 at three sites in the northern Gulf of Mexico (**Figure 1**). The first sediment trap site near the Macondo well, which we call our DWH site (also referred to as R/V Oceanus Site 26, or OC-26; 28°40'N, 88°21.6'W; at 1660 m depth) is within 5 km of the Macondo well and was

heavily impacted by the oil discharge. The site is about 70 km southeast of the Mississippi River Delta. A deployment during 2010–2011 is reported in Yan et al. (2016) and is referred to as Deployment 0 in this study. Sample collection is reported from 25 August 2010 to 29 March 2015, through five deployments of the trap (**Table 1**).

The second site, our Reference site (called AT357 by Fisher et al., 2014; 27°31.5 N, 89°42.6 W; at 1160 m depth) is located in the Atwater Valley lease block and approximates a reference or background site (Reference site; Giering et al., 2018). Here samples were collected from 16 April 2012 through 22 August 2014, through three consecutive deployments of the trap (**Table 1**). The seafloor at this site hosts a large deep-water coral population, and represents a “mineral-prone seep.” A mineral-prone seep is in the final stages of seep evolution, where the production of authigenic carbonates has blocked conduits and allowed corals to use these carbonate hard grounds for attachment surfaces (Roberts and Carney, 1997; Lapham et al., 2008a, 2008b). This categorization is consistent with the “self-sealing nature of marine seeps” (Hovland, 2002).

The third study site (Seep site) was located near a large natural hydrocarbon seep, GC-600 (27°22.5'N, 90°30.7'W; at 1380 m depth). The seep is within the Green Canyon lease block and frequently exhibits extensive oil slicks on the sea surface above it (MacDonald et al., 1993, 2002;

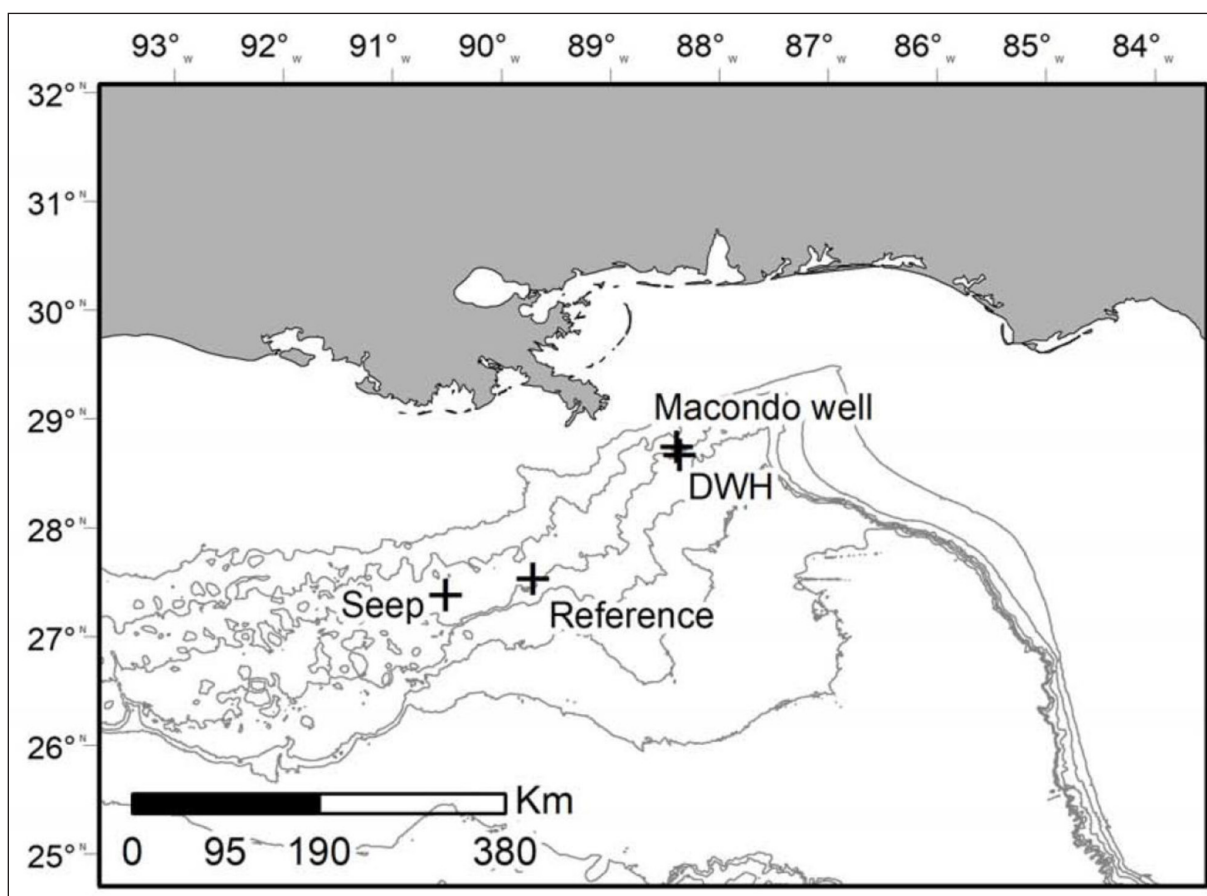


**Figure 1:** Map of our DWH, Reference and Seep sites where the sediment traps were deployed. The location of the Macondo well is also shown. Contours are 500-m water depth intervals. DOI: <https://doi.org/10.1525/elementa.298.f1>

**Table 1:** Sampling periods at the three sites and number of sampling days over each deployment period. DOI: <https://doi.org/10.1525/elementa.298.t1>

| Site | Water depth (m) <sup>a</sup> | Deployment | Start of sampling | End of sampling | Days/cup |
|------|------------------------------|------------|-------------------|-----------------|----------|
| DWH  | 1660                         | 0          | 25 Aug 2010       | 28 Sep 2011     | 21       |
| DWH  | 1660                         | 1          | 28 Jun 2012       | 8 Sep 2012      | 18       |
| DWH  | 1660                         | 2          | 12 Sep 2012       | 7 Aug 2013      | 17       |
| DWH  | 1660                         | 3          | 9 Oct 2013        | 11 Jul 2014     | 16       |
| DWH  | 1660                         | 4          | 22 Sep 2014       | 29 Mar 2015     | 17       |
| Ref  | 1160                         | 1          | 16 Apr 2012       | 11 Apr 2013     | 18       |
| Ref  | 1160                         | 2          | 5 Jun 2013        | 27 Jan 2014     | 17       |
| Ref  | 1160                         | 3          | 5 May 2014        | 22 Aug 2014     | 18       |
| Seep | 1380                         | 1          | 16 Apr 2012       | 9 Sep 2012      | 11       |
| Seep | 1380                         | 2          | 10 Sep 2012       | 29 Apr 2013     | 18       |
| Seep | 1380                         | 3          | 8 Jun 2013        | 14 Apr 2014     | 24       |
| Seep | 1380                         | 4          | 4 May 2014        | 25 Feb 2015     | 27       |
| Seep | 1380                         | 5          | 23 Apr 2015       | 18 Mar 2016     | 28       |

<sup>a</sup> Water depth at sites. Traps were deployed 120 m above the bottom at all sites. At DWH a second trap was employed at 30 m above the bottom during 2012–2013.

Garcia-Pineda et al., 2013). Sample collection is reported from 16 April 2012 to 18 March 2016, through five deployments of the trap (**Table 1**). Neither GC-600 (Seep site) nor AT357 (Reference site) was visibly impacted by hydrocarbons from the DWH spill (Fisher et al., 2014).

Traps at each of the three sites were moored 120 m above the seafloor (mab; **Table 1**), and in addition, at the DWH site, a second trap was placed 30 mab. Isotope samples were obtained over roughly a year, from 28 June 2012 from the trap 30 mab. Sinking particles were collected in time-series sediment traps as described in Yan et al. (2016) and Giering et al. (2018). Before the traps were deployed, particle collection cups were filled with filtered seawater with NaCl added to a final salinity of 40 and with HgCl<sub>2</sub> added to form a 0.14% solution to act as a preservative. The rotating carousels allowed the collection of time-sequenced samples, and each sample collected for 11–28 days (**Table 1**). After each collection period, sediment traps were recovered, sampled and redeployed immediately. The time period of each deployment is given in **Table 1**. When the sediment traps were retrieved, the preserved samples were refrigerated until processing. Samples were split into subsamples using a rotary sample splitter (WSD-10, McLane Research Laboratories). Individual splits were used for different analysis (Yan et al., 2016; Giering et al., 2018); here, we focus on δ<sup>13</sup>C, Δ<sup>14</sup>C and to a limited extent, δ<sup>34</sup>S isotopic composition.

## 2.2. Sample analysis

Prior to isotope analysis, sample splits (10% of original sample) were dried, ground, soaked briefly with 10% HCl to remove carbonates, rinsed with ultrapure water and freeze-dried. Samples were then analyzed for δ<sup>13</sup>C, Δ<sup>14</sup>C and δ<sup>34</sup>S. The δ<sup>13</sup>C was measured on a Carlo Erba elemental

analyzer coupled to a Delta XP Thermo Finnegan isotope ratio mass spectrometer. Analytical reproducibility averaged 0.2‰ based on analysis of 20 replicate samples. Stable sulfur isotopes (δ<sup>34</sup>S‰) were analyzed at the Stable Isotope Core Facility at Washington State University (Pullman, Washington). Analytical error was 0.4‰ for δ<sup>34</sup>S as reported by the facility. Results are presented relative to VPDB or CDT (δ<sup>13</sup>C or δ<sup>34</sup>S = (R<sub>sample</sub>/R<sub>std</sub> - 1) × 1000, where R = <sup>13</sup>C/<sup>12</sup>C or <sup>34</sup>S/<sup>32</sup>S).

Samples for Δ<sup>14</sup>C-POM analysis were combusted (Choi and Wang, 2004), and purified CO<sub>2</sub> prepared as graphite targets and analyzed by accelerator mass spectrometry (Vogel et al., 1984). Values are reported according to the Δ notation put forth in Stuiver and Polach (1977). The Δ notation normalizes the radiocarbon content of a sample to a nominal δ<sup>13</sup>C value (-25‰) and the collection time. The scale is linear and starts at -1000‰ when a sample has essentially 0% modern carbon which would represent petroleum residue (McNichol and Aluwihare, 2007). Analytical reproducibility of three sediment trap replicates averaged 2.8‰. Chanton et al. (2015) reported that replication of 17 sediment samples averaged 6.5‰. Samples were run on AMS facilities at Woods Hole Oceanographic Institution (NOSAMS) or the University of Georgia Center for Applied Isotope Studies. For all three isotopic scales, increases in δ (or Δ) values denote increases in the relative amount of the heavy isotope <sup>13</sup>C, <sup>14</sup>C or <sup>34</sup>S. Conversely, decreases in δ (or Δ) values denote depletion in the heavy isotope, <sup>13</sup>C, <sup>14</sup>C or <sup>34</sup>S, relative to the standard material.

Because variations in rates of photosynthesis and rates of riverine-terrestrial input can affect the isotopic composition of POM, we examined the data for correlations with the rate of particulate organic carbon (POC) flux and the rate of lithogenic particle flux, assuming that lithogenic

flux was associated with riverine inputs and/or sediment resuspension. Fluxes of POC, lithogenic materials, total particulates and polycyclic aromatic hydrocarbon (PAH) flux and composition are given in Giering et al. (2018). Lithogenic flux was calculated as dry weight – (calcium carbonate + biogenic silica +  $2.2 \times \text{POC}$ ), where the 2.2 factor converts POC to POM.

### 2.3. Statistical analysis of temporal variation

We assessed whether the time-series data for  $\delta^{13}\text{C}$ ,  $\Delta^{14}\text{C}$  and  $\delta^{34}\text{S}$  at the three sites contained any trends, autocorrelation and/or changes using the `envcpt` function of the R package `EnvCpt` (Killick et al., 2016). This function fits eight different models to the time-series data and identifies the best model fit and, if present, change points (for detailed description see R package). If the function identified change points, these were extracted (from the most likely models) and, using the median change point, a piecewise simple linear regression was performed.

We further examined the broad trends in the isotope data by considering the annual averages for the sample collection periods. We wanted to estimate how long this recovery would take by examining these grouped data, which was a second approach to the change point analysis described above. A one-way ANOVA on the  $\Delta^{14}\text{C}$  and  $\delta^{13}\text{C}$  data for all years and sites showed significant differences, which we explored using a Tukey test. At the Reference site, annual data were not different from each other ( $p$  ranged from 1.00 to 0.88); owing to the location, values at the Reference site were therefore considered typical “background” values and grouped in further Tukey tests. Inspection of the Tukey test results allowed us to place the different periods for the years and sites into three and two groups ( $\Delta^{14}\text{C}$  and  $\delta^{13}\text{C}$ , respectively) based on their similarity or, rather, their lack of significant differences. The depleted Seep site values in 2012 were defined as “Group 1” owing to the clear petrogenic signal, while the Reference site was placed in “Group 3”. Any annual data set that was not significantly different from either the Seep site in 2012 or the Reference site was placed, respectively, in “Group 1” or “Group 3”. The last group, “Group 2” for  $\Delta^{14}\text{C}$ , was intermediate between the other two groups.

For the more limited amount of  $\delta^{34}\text{S}$  data, we compared four groups of data: (1) all of the Reference site data, (2) all of the Seep site data, (3) the DWH site data for deployment 0 (Table 1), and (4) the data following deployment 0.

### 2.4. Endmember mixing model

Following Bauer et al. (2002) and Cherrier et al. (2014), we used a three-equation mixing model to estimate the percent contribution of carbon from modern surface

production, riverine and oil inputs to the sinking particulates, particularly focusing on background conditions. The following three equations, solved in a matrix system, were used:

$$R_1F_1 + R_2F_2 + R_3F_3 = R_s$$

$$C_1F_1 + C_2F_2 + C_3F_3 = C_s$$

$$S_1F_1 + S_2F_2 + S_3F_3 = S_s$$

where  $R$  represents  $\Delta^{14}\text{C}$  radiocarbon values,  $C$  represents  $\delta^{13}\text{C}$  stable isotope values and  $S$  represents  $\delta^{34}\text{S}$  stable isotope values in component  $F_1$  (surface photosynthetically fixed carbon),  $F_2$  (river-derived material), and  $F_3$  (oil-derived material). The subscript  $s$  denotes the isotopic value of the bulk sediment trap samples or their average across time spans for  $\Delta^{14}\text{C}$ ,  $\delta^{13}\text{C}$ , and  $\delta^{34}\text{S}$ .

The model has an additional constraint in that  $F_1 + F_2 + F_3$  should add up to 1, but this constraint was not forced.

The isotopic values ( $R = {}^{14}\text{C}$ ,  $C = {}^{13}\text{C}$  and  $S = {}^{34}\text{S}$ ) of the different components,  $F_1$ ,  $F_2$ , and  $F_3$  (surface production, riverine input, oil-derived, respectively) were assigned as follows. The  $\Delta^{14}\text{C}$  value of dissolved inorganic carbon in the Gulf surface waters is currently  $40.9 \pm 3.0\text{‰}$  (Chanton et al., 2012), although in subsurface layers in the upper 100 m it may have more enriched values (64‰; J. Chanton, unpublished data). Recent marine photosynthetic carbon reflects this  $\Delta^{14}\text{C}$  value; plankton collected in the Gulf from 2010 to 2014 (J. Chanton and S. Bosman, unpublished data) had a  $\Delta^{14}\text{C}$  of  $38.8 \pm 25.8\text{‰}$  ( $n = 79$ ; Table 2). We used  $38.8 \pm 25.8\text{‰}$  to represent  $R_1$ . Similarly,  $\delta^{13}\text{C}$  values of Gulf plankton collected from 2010 to 2014 have a  $\delta^{13}\text{C}$  of  $-21.2 \pm 1.5\text{‰}$  ( $C_1$ ,  $n = 82$ ; J. Chanton and S. Bosman, unpublished data) similar to the values measured by Chanton and Lewis (2002) of 22 to  $-20\text{‰}$ . The  $\delta^{34}\text{S}$  isotopic composition of plankton in the Gulf is  $20 \pm 1.0\text{‰}$  ( $S_1$ ,  $n = 15$ ; J. Chanton and S. Bosman unpublished data), similar to seawater sulfate isotopic composition (Rees et al., 1978), indicating non-fractionating assimilatory sulfate reduction of marine sulfate to form organic sulfur.

Riverine POM associated with the outflow from the Mississippi River is somewhat depleted in both carbon isotopes and has been reported to range from  $-86$  to  $-223\text{‰}$  for  $\Delta^{14}\text{C}$  and  $-23.3$  to  $-26.0\text{‰}$  for  $\delta^{13}\text{C}$  (Chanton et al., 2015). Rosenheim et al. (2013) reported bulk Mississippi River POM during a high discharge event in 2008 at a  $\Delta^{14}\text{C}$  of  $-226 \pm 7\text{‰}$ , and during a lower discharge year in 2009 at  $-107.2 \pm 40\text{‰}$ . Atchafalaya River POM during the lower discharge year 2009 had a  $\Delta^{14}\text{C}$  of  $-175 \pm 46\text{‰}$

**Table 2:** Endmember isotopic values used for the mixing model. DOI: <https://doi.org/10.1525/elementa.298.t2>

| Source                      | $\Delta^{14}\text{C}\text{‰}$ | $\delta^{13}\text{C}\text{‰}$ | $\delta^{34}\text{S}\text{‰}$ |
|-----------------------------|-------------------------------|-------------------------------|-------------------------------|
| Marine primary production   | $39 \pm 26$                   | $-21.2 \pm 1.5$               | $20.0 \pm 1.0$                |
| Riverine-terrestrial inputs | $-154 \pm 68$                 | $-24.6 \pm 1.3$               | $0 \pm 5$                     |
| Fossil carbon (oil)         | $-1000$                       | $-27.0 \pm 0.3$               | $-10 \pm 5$                   |

(Rosenheim et al., 2013). We used a mid-point of the ranges given above for riverine POM,  $-154 \pm 68\text{‰}$  for  $\Delta^{14}\text{C}$  ( $R_2$ ) and  $-24.6\text{‰}$  for  $\delta^{13}\text{C}$  ( $C_2$ ) (**Table 2**). For  $\delta^{34}\text{S}$  we used a value of  $0 \pm 5\text{‰}$  ( $S_2$ ; Chanton and Lewis, 2002).

Oil emanating from hydrocarbon seepage or the oil spill has a  $\Delta^{14}\text{C}$  value of  $-1000\text{‰}$  ( $R_3$ ) and a  $\delta^{13}\text{C}$  values of  $-27 \pm 0.3\text{‰}$  ( $C_3$ ; Graham et al., 2010). Because such material is known to bear a depleted  $\delta^{34}\text{S}$  signature due to the influence of dissimilatory sulfate reduction and the subsequent interaction of sulfide with organic matter, we used a  $\delta^{34}\text{S}$  value of  $-10 \pm 5\text{‰}$  ( $S_3$ ; Chanton et al., 1987). Endmember isotopic values are summarized in **Table 2**. We performed a sensitivity test on the model by varying the input parameters according to their uncertainty reported in **Table 2**. We neglected methane inputs in this calculation (Chanton et al., 2012; Cherrier et al., 2014) because the pulse of methane was likely rapidly consumed in the water column (Crespo-Medina et al., 2014) and to simplify the model. In addition, the uptake of the methane pulse in the system was microbially dominated, and likely contributed more to the smaller sized suspended POM (Cherrier et al., 2014) rather than to the larger sinking particles considered here. The effect of including methane in this model would have resulted in less organic carbon being attributed to hydrocarbon (petrocarbon) inputs.

### 3. Results

#### 3.1. Time series of isotopic tracers

Time-series isotope results for sinking POM ( $\text{POM}_{\text{sink}}$ ) at the three sites (DWH, Reference and Seep sites) are presented in **Figure 2**; the individual sampling/deployment

periods are given in **Table 1**. As discussed above, the more sensitive indicator,  $\Delta^{14}\text{C}$ , varied from  $-180\text{‰}$  to  $93\text{‰}$  at the DWH site,  $-52\text{‰}$  to  $66\text{‰}$  at the Reference site, and  $-200\text{‰}$  to  $62\text{‰}$  at the Seep site.

At the DWH site, the first three sample cups (1–3) had conspicuously high isotope values for  $\Delta^{14}\text{C}$  and  $\delta^{34}\text{S}$  (**Figure 2**). These high values are linked to the unusually high flux dominated by a phytoplankton bloom collected at that time (see Giering et al., 2018; Yan et al., 2016). We therefore excluded the first three cups from the trend analysis for  $\Delta^{14}\text{C}$ . For  $\Delta^{14}\text{C}$ , we observed depleted values starting in October 2010, followed by an increase over the sampling period and a change point around in July 2013. During this period, maximum  $^{14}\text{C}$  depletion was observed on 8 December 2010, and this time point is used to represent this period in mixing model calculations below. Piecewise regression over this time period, excluding the first three cups, showed that  $\Delta^{14}\text{C}$  increased from depleted values at a rate of  $0.07 \pm 0.02\text{‰ d}^{-1}$  until July 2013, though variability was high ( $p < 0.01$ ;  $R^2 = 0.47$ ,  $n = 40$ ). Thereafter, there was no trend over time and the mean  $\Delta^{14}\text{C}$  value ( $-3.2 \pm 31.0\text{‰}$ ; **Table 3**) was similar to the  $\Delta^{14}\text{C}$  value at the Reference site ( $3.8 \pm 31.1\text{‰}$ ). For  $\delta^{13}\text{C}$ , there was no significant trend with time ( $p = 0.19$ ) or change point, and the mean was  $-21.9 \pm 0.5\text{‰}$  (**Table 3**).

For  $\delta^{34}\text{S}$ , following the first three time points, values between 27 October 2010 and 7 September 2011 were low (mean  $7.4 \pm 3.1\text{‰}$ ). Between November 2012 and March 2015, the mean  $\delta^{34}\text{S}$  was much higher ( $16.9 \pm 2.0\text{‰}$ ). Because of the data gap, it is not clear whether this was a gradual increase or a step change, though we believe the

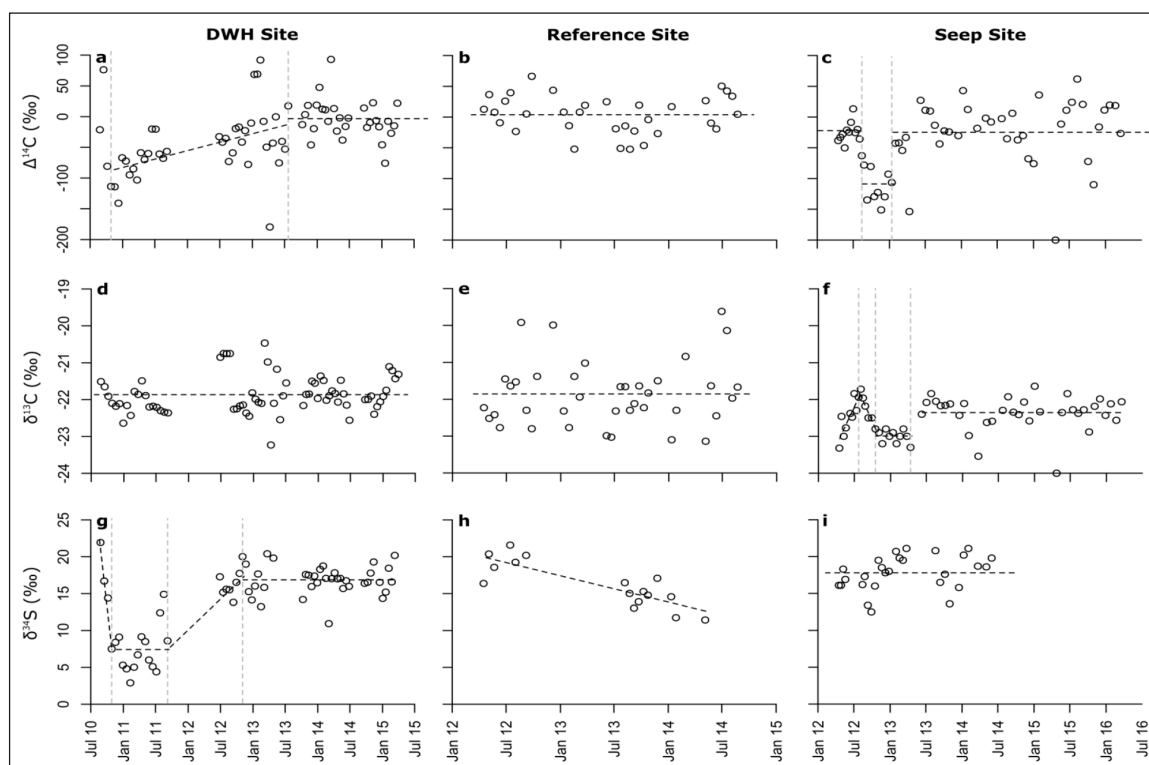


**Figure 2: Time series of  $\delta^{13}\text{C}$ ,  $\Delta^{14}\text{C}$  and  $\delta^{34}\text{S}$  isotope data from the sediment trap deployments.** Shown are data from our Reference, Seep and DWH sites, fit by EnvCpt (Killick et al., 2016) to find change points in the data. DOI: <https://doi.org/10.1525/elementa.298.f2>

**Table 3:** Isotopic results for particle collection periods used for 3-endmember mixing model assessment, with model results assigning the source components to be marine primary production (marine), riverine-terrestrial inputs (riverine) and fossil carbon (oil). DOI: <https://doi.org/10.1525/elementa.298.t3>

| Site, condition                         | Isotope values                |                               |                               | Model results assigning source <sup>a</sup> |                 |                 |                  |
|---|-------------------------------|-------------------------------|-------------------------------|---|-----------------|-----------------|------------------|
|   | $\Delta^{14}\text{C}\text{‰}$ | $\delta^{13}\text{C}\text{‰}$ | $\delta^{34}\text{S}\text{‰}$ | Marine                                      | Riverine        | Oil             | Sum <sup>b</sup> |
| DWH site, depleted values<br>8 Dec 2010 | -141.0                        | -22.1                         | 9.1                           | $0.51 \pm 0.07$                             | $0.34 \pm 0.15$ | $0.11 \pm 0.03$ | 0.96             |
| DWH site, after July 2013               | $-3.2 \pm 31.0$               | $-21.9 \pm 0.5$               | $16.9 \pm 2.0$                | $0.85 \pm 0.09$                             | $0.14 \pm 0.07$ | $0.01 \pm 0.01$ | 0.99             |
| Reference site, average                 | $3.8 \pm 31.1$                | $-21.9 \pm 0.9$               | $16.2 \pm 3.1$                | $0.81 \pm 0.08$                             | $0.20 \pm 0.08$ | $0.00 \pm 0.03$ | 1.01             |
| Seep site, non-trough                   | $-21.7 \pm 45.7$              | $-22.3 \pm 0.5$               | $18.4 \pm 2.1$                | $0.95 \pm 0.05$                             | $0.03 \pm 0.05$ | $0.05 \pm 0.03$ | 1.03             |
| Seep site, trough                       | $-109.0 \pm 29.1$             | $-23.0 \pm 0.2$               | $16.6 \pm 2.3$                | $0.90 \pm 0.05$                             | $0.0 \pm 0.06$  | $0.14 \pm 0.03$ | 1.04             |

<sup>a</sup>The isotopic composition of these source terms is given in Table 2.

<sup>b</sup>The sum of the different predicted source fractions, which should equal 1, is within 4% of 1.0 or better.

former is more likely based on the  $\Delta^{14}\text{C}$  data. Assuming a linear increase,  $\delta^{34}\text{S}$  increased at a rate of  $\sim 0.023\text{‰ d}^{-1}$ . For all three isotopes, including autoregression (influence from preceding sample) provided a better fit, meaning that often data points closely followed each other. The mean values for the DWH site for post-July 2013 and the representative time point of 8 December 2010 are given in **Table 3** and are used in subsequent calculations.

Change point analysis of the  $\Delta^{14}\text{C}$  values for  $\text{POM}_{\text{sink}}$  at the Reference site did not show any significant trends over time ( $p = 0.69$ ; **Figure 2**), though there appeared to be a weak autoregression (influence from preceding sample). The mean of the observed values was  $3.8 \pm 31.1\text{‰}$  (**Table 3**). At the Reference site,  $\delta^{13}\text{C}$  time-series data also showed no change over time. The change point analysis indicated that the best model fit was a constant mean ( $-21.9 \pm 0.9\text{‰}$ ), which was confirmed by linear regression (no significant trend;  $p = 0.51$ ).  $\delta^{34}\text{S}$  at this site was high in 2012 and lower in 2013/2014. However, because of a gap in the data, we have no information on whether this pattern was caused by a constant decrease or a sudden step change.  $\delta^{34}\text{S}$  values had an overall mean of  $16.2 \pm 3.1\text{‰}$  (**Table 3**).

At the Seep site, change point analysis of the  $\Delta^{14}\text{C}$  time series indicated a period of significant isotopic depletion, a “trough”, from 14 August 2012 to 13 January 2013 (**Figure 2**). During this trough period,  $\Delta^{14}\text{C}$  was on average  $-109.0 \pm 29.1\text{‰}$ . Before and after this period, values were considerably enriched (mean of  $-21.7 \pm 45.7\text{‰}$ ; **Table 3**). There was one unusually low observation for the cup that commenced sampling on 23 April 2015 ( $-200.1\text{‰}$ ). For  $\delta^{13}\text{C}$ , there were definite isotopic shifts in the beginning of the time series with an increase in the first cups (until around 23 July 2012), followed by a steep decrease starting in August 2012 and a trough (mean of  $-23.0 \pm 0.2\text{‰}$ ), followed by a rise and relatively stable period from June 2013 onwards (mean of  $-22.3 \pm 0.5\text{‰}$ ). There were two unusually low  $\delta^{13}\text{C}$  values for the cups that commenced sampling on 23 March 2014 and 23 April 2015 ( $-23.5$  and  $-24.0\text{‰}$ , respectively).  $\delta^{34}\text{S}$  values were relatively constant over the entire time series, averaging  $17.8 \pm 2.3\text{‰}$ . The mean of the  $\delta^{34}\text{S}$  trough was  $16.6 \pm 2.3\text{‰}$ , while non-trough values were on average  $18.4 \pm 2.1\text{‰}$  (**Table 3**).

### 3.2. Flux at 120 versus 30 m above the bottom

At the DWH site, there was excellent correspondence in both  $\Delta^{14}\text{C}$  and  $\delta^{13}\text{C}$  between the trap material ( $\text{POM}_{\text{sink}}$ ) collected 120 m above the seafloor (mab) relative to the material collected 30 mab (**Figure 3**). This correspondence indicates good reproducibility of our measurements and that both traps were capturing similar source material. For the  $\Delta^{14}\text{C}$  data, values from both traps correlated significantly (linear regression: slope = 0.98, intercept =  $23.1\text{‰}$ ,  $p = 0.001$ ,  $r = 0.81$ ,  $n = 22$ ). For the  $\delta^{13}\text{C}$  data, the correlation between both traps was similarly strong (linear regression: slope = 1.2, intercept =  $3.5\text{‰}$ ,  $p < 0.0001$ ,  $r = 0.96$ ,  $n = 22$ ). The two regressions both had slopes near 1 indicating strong co-variance across time in the data from the bottom (30 mab) and off-bottom (120 mab) traps; however, there was a systematic offset in  $\Delta^{14}\text{C}$  between the two traps with lower isotopic values in the bottom trap. This is reflected by the intercept of the linear regression ( $23.1\text{‰}$ ) and paired T-tests, directly comparing the isotope data for each date, which showed a significant difference between the top and bottom trap ( $n = 22$ ,  $p = 0.017$ ). The mean for the 30 mab trap was  $-52 \pm 38\text{‰}$ , while the mean for the 120 mab trap was  $-28 \pm 58\text{‰}$ . The difference in means ( $24\text{‰}$ ) was similar to the intercept for the linear regression ( $23.1\text{‰}$ ). For  $\delta^{13}\text{C}$ , the paired T-test indicated no significant difference between the two traps ( $-21.6 \pm 0.6\text{‰}$  and  $-21.8 \pm 0.7\text{‰}$ ). Comparing  $\delta^{34}\text{S}$  values between the two traps, there was no significant correlation between the 120 mab and 30 mab traps ( $r = 0.56$ ,  $n = 10$ ,  $p = 0.09$ ), which was supported by a paired T-test also indicating no significant differences between the material in the two traps.

### 3.3. Similarities in isotopic signature between the sites

Isotope cross-plots of  $\Delta^{14}\text{C}$  versus  $\delta^{13}\text{C}$  at the three sites clearly show the temporal variability in isotopic signature of sinking material (**Figure 4**). At the DWH site (**Figure 4**), sinking particles collected shortly after the DWH spill are isotopically depleted, but sinking material became enriched throughout the sampling period and more similar to values observed at the Reference Site (grey

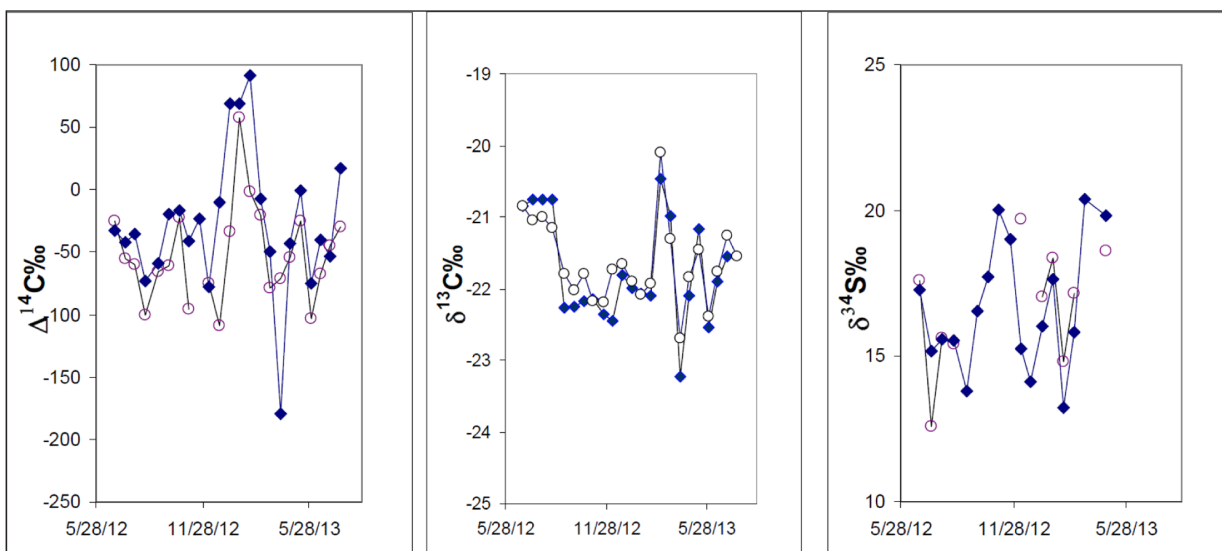


**Figure 3: Time series of  $\delta^{13}\text{C}$ ,  $\Delta^{14}\text{C}$  and  $\delta^{34}\text{S}$  data at two depths at the DWH site.** Shown are data from traps deployed at 30 m (open circles) and 120 m (solid diamonds) above the seafloor. Dates indicate month/day/year. DOI: <https://doi.org/10.1525/elementa.298.f3>

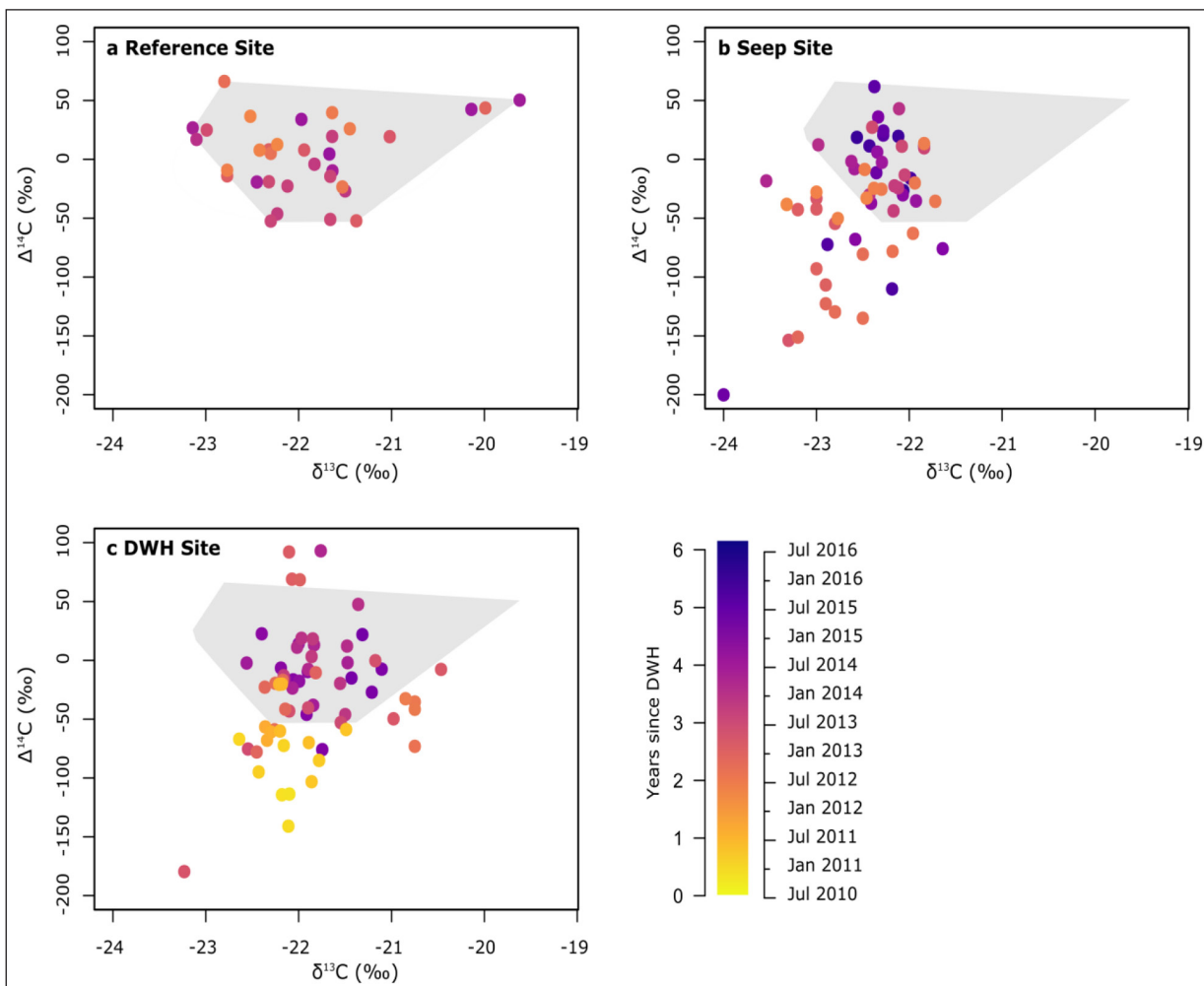


**Figure 4: Isotope cross-plots organized by site years (color scale) since the DWH oil spill.** Panel a presents the data from the Reference site (AT-357). The isotope space occupied by the data is fit with a grey polygon which is carried into panels b and c. Panel b presents the data from the Seep site (GC-600). Note the displacement to the lower left field in the graph which occurred in late 2012 (2–3 years after the spill). Panel c presents the data from the DWH site (OC-26). Following the oil spill, values were displaced to the lower left field but had returned to background values by July 2013 (3 years after the spill). DOI: <https://doi.org/10.1525/elementa.298.f4>

polygons in **Figure 4**). For the Reference site, the isotope cross-plot indicates that most samples are closely clustered; i.e., sinking material was similar and did not change isotopically with time (**Figure 4**). At the Seep site, fluxes were clearly depleted in  $^{13}\text{C}$  and  $^{14}\text{C}$  during 2012 (relative to the Reference site), but were similar to the Reference Site later during our study period (**Figure 4**).

These trends were confirmed by our statistical groupings. Based on annual means from 2010 through 2013, sinking material at the DWH site showed more depleted  $\Delta^{14}\text{C}$  values than sinking material at the Reference site. The differences in isotopic signature between the two sites were significant ( $p < 0.05$ ) in 2010 and 2011 (Group 1; **Table 4**). By 2012, fluxes at the DWH site were not significantly different isotopically from the Reference site (Group 3), though the mean was much lower than at the Reference Site ( $-39.2 \pm 22.5\%$  vs  $3.8 \pm 31.1\%$ , respectively). In 2012 and 2013, the DWH values were not different from the DWH values in 2010 or 2011 either, so they are placed in Groups 1 and 3. By 2014, the DWH site was significantly different from previous years (2010–2013) at the DWH site, and was similar to the Reference site, as indicated by the identical mean and standard deviation (Group 3 only; **Table 4**).  $\Delta^{14}\text{C}$  values at the Seep site indicated that 2013, 2014 and 2015 were not significantly different from the Reference site (Group 3), nor were they different from the DWH values in 2010–2014 (Group 1 and Group 2); thus, they fit into all three groups. Group 2 includes the DWH sampling in years 2010–2013, but does not include the Seep site in 2012 because there was a significant difference between the DWH site in 2013 and the Seep site in 2012.

The  $\delta^{13}\text{C}$  data were placed into only two groups (Groups 1 and 3) based on differences in the data. Deployments in 2010 and 2011 at the DWH site were similar to the Seep site (Group 1; **Table 4**). However, throughout the study period, DWH site  $\delta^{13}\text{C}$  values were not different from the Reference site (Group 3; **Table 4**). In terms of  $\delta^{13}\text{C}$ , the Seep site was significantly different from the Reference site during 2012, 2013 and 2014 (Group 1; **Table 4**), but was not significantly different from the Reference site in

2015 (Group 3; **Table 4**). For  $\delta^{34}\text{S}$ , all of the means were similar except for the DWH site in 2010, which was significantly different ( $p < 0.01$ ).

### 3.4. Relationship of isotopic composition to POC and lithogenic flux

The  $\Delta^{14}\text{C}$  of the sinking matter and its POC flux (Giering et al., 2018) was not correlated at any of the sites. At the DWH site,  $\Delta^{14}\text{C}$  of sinking material was also not correlated with lithogenic particle flux (Giering et al., 2018). At the Reference and Seep sites, on the other hand,  $\Delta^{14}\text{C}$  and lithogenic flux were significantly negatively correlated (Reference site:  $p = 0.035$ ,  $r = 0.374$ ,  $n = 32$ ; Seep site:  $p < 0.001$ ,  $r = 0.428$ ,  $n = 60$ ; **Figure 5**). At the Reference site, this correlation was driven by two points at one extreme and a cluster near the origin of the graph (data not shown). At the Seep site, the most depleted  $\Delta^{14}\text{C}$  values occurred at lithogenic flux values between 150 and 300  $\text{mg m}^{-2}\text{d}^{-1}$  (**Figure 5**). When plotted against time, the inverse relationship between lithogenic flux and depleted  $\Delta^{14}\text{C}$  at the Seep site was obvious (**Figure 5**). In terms of  $\delta^{13}\text{C}$ , the  $\delta^{13}\text{C}$  of collected material at the DWH site was positively correlated (became  $^{13}\text{C}$  enriched) with both increasing POC flux ( $r = 0.34$ ,  $n = 70$ ,  $p = 0.004$ ) and increasing lithogenic particle flux ( $r = 0.33$ ,  $n = 70$ ,  $p = 0.005$ ). At the Reference and Seep sites, there was no correlation between  $\delta^{13}\text{C}$  and the POC flux.

### 3.5. Baseline and source contribution to organic material

The isotopic values assigned to the different input terms (**Table 2**) and the particulates over different collection times (**Table 3**) are graphed in **Figure 6** in three-dimensional space for  $\Delta^{14}\text{C}$ ,  $\delta^{13}\text{C}$  and  $\delta^{34}\text{S}$ . The symbols representing the collected particulates under “background” conditions, DWH site after July 2013, Reference site, and Seep site “non-trough”, all cluster near the marine endmember in the graph and clearly demonstrate the importance of modern marine photosynthetic production. The Seep site “trough” and DWH site 2010 data trend down and left towards the river and hydrocarbon

**Table 4:** Mean and standard deviation (SD) for  $\delta^{13}\text{C}\%$  and  $\Delta^{14}\text{C}\%$  for each sampling year with results of 1-way ANOVA followed by Tukey test. DOI: <https://doi.org/10.1525/elementa.298.t4>

| Site <sup>a</sup> | Year      | $\Delta^{14}\text{C}\%$ |      |    | $\delta^{13}\text{C}\%$ |     |    | Groups <sup>b</sup> |                 |
|-------------------|-----------|-------------------------|------|----|-------------------------|-----|----|---------------------|-----------------|
|                   |           | Mean                    | SD   | n  | Mean                    | SD  | n  | $^{14}\text{C}$     | $^{13}\text{C}$ |
| Ref               | 2012–2014 | 3.8                     | 31.1 | 33 | -21.9                   | 0.9 | 38 | 3                   | 3               |
| DWH               | 2010      | -66.0                   | 73.7 | 7  | -22.0                   | 0.4 | 7  | 1, 2                | 1, 3            |
| DWH               | 2011      | -64.2                   | 25.2 | 12 | -22.1                   | 0.3 | 12 | 1, 2                | 1, 3            |
| DWH               | 2012      | -39.2                   | 22.5 | 11 | -21.7                   | 0.7 | 11 | 1, 2, 3             | 3               |
| DWH               | 2013      | -13.4                   | 61.9 | 18 | -21.8                   | 0.6 | 17 | 2, 3                | 3               |
| DWH               | 2014      | 4.3                     | 30.4 | 17 | -21.9                   | 0.3 | 17 | 3                   | 3               |
| Seep              | 2012      | -62.7                   | 49.1 | 20 | -22.5                   | 0.5 | 19 | 1                   | 1               |
| Seep              | 2013      | -37.0                   | 46.8 | 14 | -22.5                   | 0.5 | 14 | 1, 2, 3             | 1               |
| Seep              | 2014      | -12.8                   | 29.7 | 11 | -22.5                   | 0.4 | 14 | 1, 2, 3             | 1               |
| Seep              | 2015      | -26.8                   | 74.7 | 12 | -22.4                   | 0.6 | 12 | 1, 2, 3             | 1, 3            |

<sup>a</sup> DWH 2015 and Seep 2016 were not included in this analysis because of a small number of samples.

<sup>b</sup> Groups represent data that were not significantly different from each other (see Section 2.3).

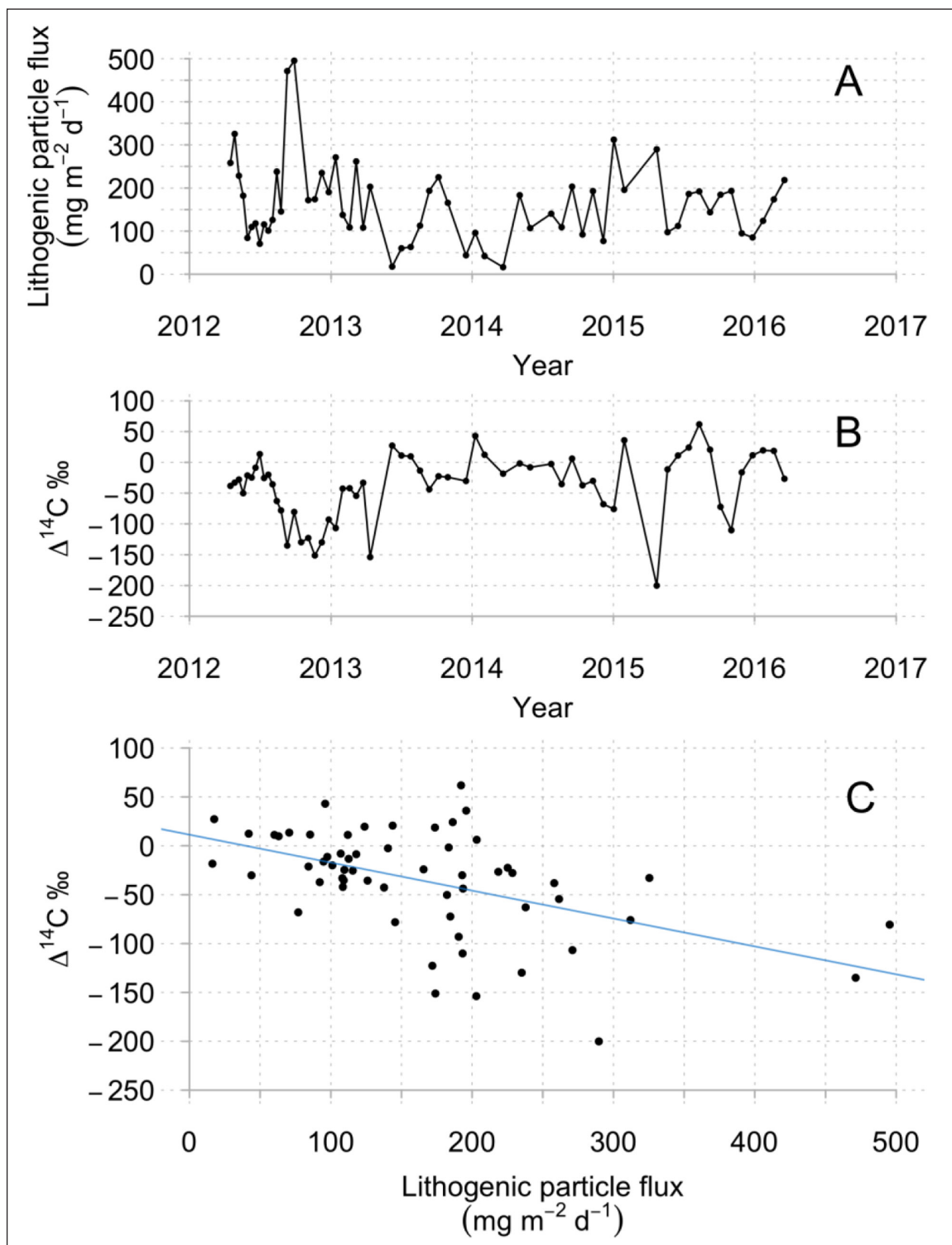


**Figure 5: Relationships between lithogenic flux and  $\Delta^{14}\text{C}$ ‰ at the Seep site (GC 600).** Upper panels **A** and **B** present time series; lower **panel C**, linear relationship. DOI: <https://doi.org/10.1525/elementa.298.f5>

endmembers. Based on values assigned to the different sites and collection periods presented in Section 3.1 and summarized in **Table 3**, and the values assigned to the different input terms as described in Methods Section 2 (and **Table 2**) using the 3-endmember mixing model, we calculated that under background conditions, marine primary production dominated carbon inputs at the DWH site after July 2013 and at the Reference site, from  $0.85 \pm 0.09$  to  $0.81 \pm 0.08$ , respectively (**Table 3**). Uncertainty

derives from the variation of the input parameters and the uncertainty about the means of the results. At the Seep site, which was further west of the river mouth and further from shore than the other two sites, marine production was estimated to be  $0.95 \pm 0.05$  under non-trough and  $0.90 \pm 0.05$  under trough conditions.

Riverine carbon was the dominant secondary source at the DWH and Reference sites, and ranged from  $0.14 \pm 0.07$  during background conditions at the DWH Site to

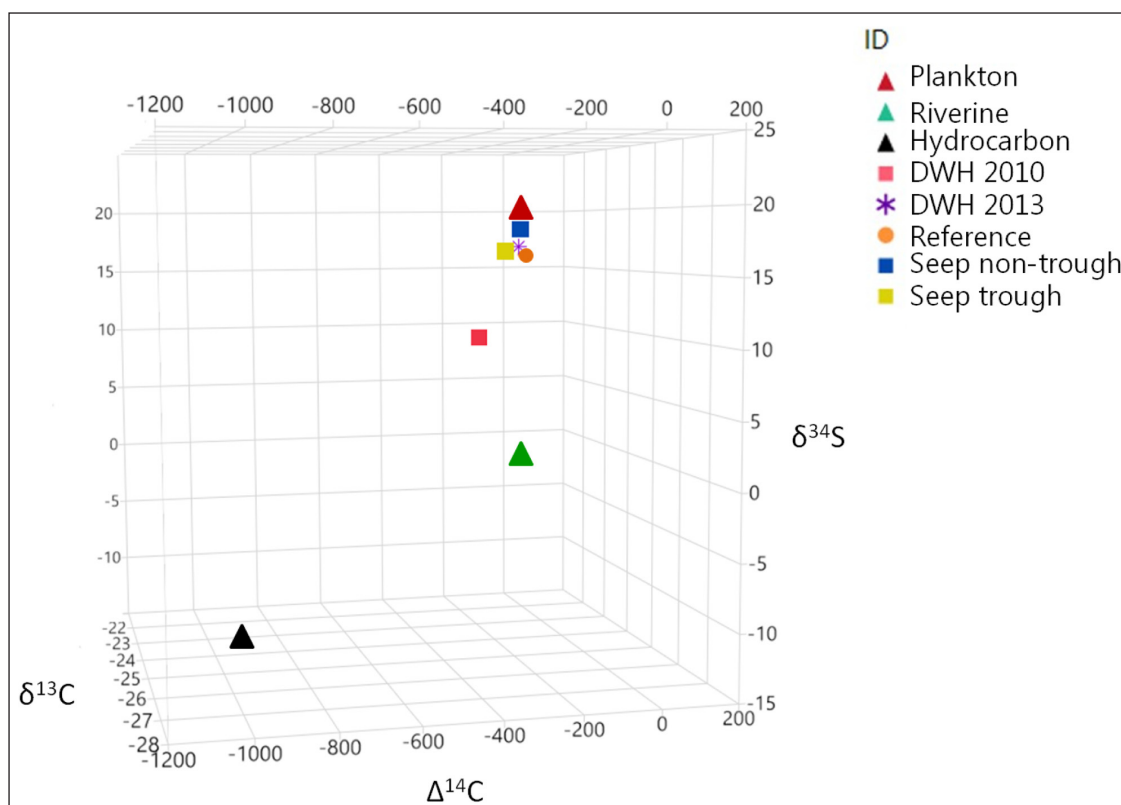


**Figure 6: Three-dimensional graph of organic matter sources and sites/time periods.** Sources are marine production (red triangle), river-derived (green triangle), and petrocarbon (black triangle). Averages at different sites and time periods are shown for the DWH site in December 2010 (red square), DWH site after 2013 (purple star), Reference site (orange circle), Seep site non-trough (blue square), and Seep site trough (yellow square). DOI: <https://doi.org/10.1525/elementa.298.f6>

$0.20 \pm 0.08$  at the Reference site. In 2010, riverine carbon was estimated to be  $0.34 \pm 0.15$  at the DWH Site, using the depleted values obtained in December (**Table 3**). At the Seep site, riverine inputs were estimated to be less important, at only  $0.03 \pm 0.05$ .

Hydrocarbon inputs during 2010 at the DWH were estimated to be as much as  $0.11 \pm 0.03$  of carbon inputs. At the seep site hydrocarbon inputs were estimated to be  $0.14 \pm 0.03$  during the trough conditions, and  $0.05 \pm 0.03$  during Seep site background or non-trough conditions. Hydrocarbon inputs at the Seep site were higher than at the DWH and Reference sites under background conditions ( $0.01 \pm 0.01$  and  $0.0 \pm 0.03$ , respectively; **Table 3**). The input estimates summed to be within 4% of 1.

## 4. Discussion

### 4.1. Recovery in isotopic composition of sinking particles at the DWH site

Our first objective was to use the temporal trend in the isotopic composition of sinking particles to determine the recovery time of the northern Gulf of Mexico after the DWH oil spill. We observed depleted  $^{14}\text{C}$  and  $^{34}\text{S}$  in sinking particles at the DWH site following the oil spill. Similar observations were made at a nearby site by Prouty et al. (2016) who observed sinking POM to be depleted in both  $^{34}\text{S}$  and  $^{14}\text{C}$  following the spill relative to pre-spill values. Our observed  $\Delta^{14}\text{C}$  values at the DWH Site were initially (in 2010) similar to the most depleted values collected

at the natural seep site. Over time, the  $\Delta^{14}\text{C}$  composition of the  $\text{POM}_{\text{sink}}$  at the DWH site became increasingly  $^{14}\text{C}$ -enriched at a rate of  $0.07\text{‰}$  per day ( $25\text{‰}$  per year) until July 2013 (**Figure 2**). After July 2013, the  $\Delta^{14}\text{C}$  values became indistinguishable from the isotopic composition of sinking POM at the Reference site (**Figure 2; Table 3**). Thus, our data suggest that the recovery of the Gulf in the vicinity of our sites (**Figure 1**), in terms of the  $^{14}\text{C}$  composition of sinking particulates, took a period of three years, from the date of the capping of the well in July 2010 to July 2013. The  $\delta^{34}\text{S}$  data for the DWH site indicated that the ecosystem recovered (in terms of sinking particulate inputs) sometime between September 2011 and November 2012, 1.2 to 2.3 years after the spill. Both estimates agree well with the estimated recovery for particulates in the northern Gulf over a period of about 2 years, based on our interpretation (see below) of the hydrocarbon composition data which was presented by Giering et al. (2018), and 1 year by Stout and Passow (2015).

These differences in apparent recovery times are driven by the sensitivity of the indicators, their relative quantities in the particulate material, and the possibility that the indicators are reflecting the recovery of differing processes. That equilibria are reached at different speeds for differing processes is not surprising. For example, in terms of floating surface oil, the recovery period was weeks following the spill (MacDonald et al., 2015). Regarding the presence of drilling muds in sinking material, the recovery

time was in months (Yan et al., 2016). Microbial populations should recover faster than sea birds and sea mammals, as generation times differ. On the whole, we should expect recovery estimates of different indicators at different rates.

Yan et al. (2016) reported that, although hydrocarbons from the DWH event were mostly undetectable in Gulf waters a few weeks after the well was capped, hydrocarbon markers absorbed to sinking particles were detectable for several months (until the beginning of 2011). Likely, the sinking marine snow acted as an accumulator of oil compounds dispersed at low concentrations in the water column, and stripped the water column of these contaminants. This interpretation is consistent with our observations that, in the days following the large sedimentation event in fall 2010, markers for oil compounds in sedimented material (depleted  $^{14}\text{C}$  and  $^{34}\text{S}$  values) were indeed low for some time, but increased again as lateral advection and mixing replenished oil compounds in the water (**Figure 4**). Fingerprinting of the oil compounds in the trap revealed that DWH oil sedimented until August 2011, for a full year after the well was capped (Stout and Passow, 2015). After 2011, the PAH indices, carbon preference index, and other indicators of hydrocarbon contamination in sinking POM were indistinguishable from background values (Yan et al., 2016). In 2012–2013, PAH fluxes were orders of magnitude lower in the northern Gulf than they were during the oil spill (Adhikari et al., 2015). Sinking particles are a significant sink for PAHs from the water column (Bouloubassi et al., 2006).

Giering et al. (2018) presented data on the PAH composition of material collected at our sites which we can compare to our isotopic data. As a simple metric, we used the relative contribution of phenanthrene to total measured PAH. Phenanthrene is used to indicate greater pyrogenic (combustion) than petrogenic (crude oil) sources (Alberty and Reif, 1988). At our Reference site, phenanthrene generally made up the bulk of the PAH flux over the entire measurement period, which we interpret as “background” or relatively unaffected particulate flux (Figure S4 in Giering et al., 2018). At the Seep site, phenanthrene was generally the dominant PAH (Figure S3 in Giering et al., 2018) except during periods when hydrocarbon contamination associated with the hydrocarbon seepage. Thus, according to our metric, background conditions were indicated when phenanthrene made up the bulk of the PAH flux. At the DWH trap, phenanthrene composed roughly 15% of the PAH flux from 25 August 2010 to 23 March 2011 (Figure S2 in Giering et al., 2018). In May 2011, it increased to about 25% of the total PAH composition, and by 2012, it further increased to as much as 50% of the PAH composition. We interpret these results to indicate a recovery time of about 2 years. Consistent with this interpretation, we found a significant correlation between  $^{14}\text{C}$  enrichment, indicating system recovery, and the percentage contribution of phenanthrene to total PAH flux across all three sites ( $r = 0.324$ ,  $n = 67$ ,  $p = 0.0075$ ).

While these studies suggest that the spilled oil was lost from the ecosystem relatively quickly (by 2012), our isotopic data indicate that some of the oil-derived elements

(such as carbon) were still sedimenting up to July 2013. Our observed enrichment in  $^{14}\text{C}$  at the DWH site over time was likely driven by changes in the quantity and quality of petrocarbon in the sinking particles: as petrocarbon was remineralized and scavenged from the water, and the water column became “cleansed”, the ‘younger’ (in terms of carbon age, enriched in terms of  $\Delta^{14}\text{C}$ ) the sedimenting material became. In addition, some oil was likely broken down by microbes and incorporated into biomass, which then circulated in the pelagic ecosystem for some time. The radiometric analysis reveals these spill-derived compounds until July 2013, when spill-derived PAHs were below detection limit. The  $\delta^{34}\text{S}$  values tell a similar story. Depleted  $\delta^{34}\text{S}$  values are associated with dissimilatory sulfate reduction (Chanton et al., 1987), which can occur when organic compounds are exposed to hydrogen sulfide in a subsurface petroleum reservoir. The observed  $\delta^{34}\text{S}$  depletion in 2010–2011 is consistent with incorporation of petrocarbon and petrocarbon-derived biomass into sinking particles. Following this interpretation, our data indicate that petrocarbon from the spill was a component in sinking material at the DWH site until early to mid-2013 (**Figure 2**).

#### 4.2. Riverine influences at the DWH Site

In response to the DWH incident, the Mississippi River floodgates were opened to push the oil away from the Mississippi Delta marshlands. The released river water would carry large amounts of nutrients, organic matter and fine lithogenic particles to offshore regions. Our mixing model calculations (**Table 3**) indicated an increase in delivery of both riverine ( $34 \pm 15\%$ ) and oil carbon ( $11 \pm 3\%$ ) during the 2010 period at the DWH site, consistent with the opening of the coastal floodgates to release river water to drive the oil offshore, and with the oil release during the DWH event. Even after July 2013, the riverine influence was marked at the DWH site ( $\sim 14 \pm 7\%$  of C; **Table 3**), suggesting that this site is strongly influenced by riverine inputs. We further observed a strong correlation between POC flux, lithogenic matter flux and  $\delta^{13}\text{C}$  enrichment, suggesting that these three parameters are linked at the DWH Site (see Section 3.4).

$\delta^{13}\text{C}$  behaves differently than  $\Delta^{14}\text{C}$ : enrichment of  $\delta^{13}\text{C}$  can be caused by enhanced primary production, because at higher photosynthetic rates less isotopic fractionation occurs with respect to dissolved inorganic carbon during carbon fixation. In addition, enhanced nutrient concentration can result in larger phytoplankton cells which are also associated with increasing  $^{13}\text{C}$  enrichment (Laws et al., 1995; Bidigare et al., 1997; Rau et al., 1997; Burkhardt et al., 1999). The observed correlations between  $\delta^{13}\text{C}$  and both lithogenic flux and POC flux hence suggest that increased lithogenic flux and POC fluxes were related to increased primary production at this site. Particle flux at the DWH site has been suggested to be closely linked to Mississippi River discharge, which supplies nutrients that enhanced primary production (Giering et al., 2018). Our observations further strengthen this idea that the primary effect of the river plume on  $^{13}\text{C}$  variability at the DWH site was nutrient addition which served to enhance primary production.

### 4.3. Resuspension

Our isotope data could have been influenced by resuspension, which could deplete isotopic signatures through the incorporation of 'aged' material. Diercks et al. (2018) provide evidence for resuspension affecting the sediment traps at the DWH site in two ways, via lateral transport and via stirring off of the bottom. Lateral transport would be more likely to affect the upper 120 mab trap, while stirring off the bottom would more likely affect the lower 30 mab trap (**Figure 3**). While differences in  $\Delta^{14}\text{C}$  between the two traps were minor, because the bulk of organic carbon in the traps originated from sinking surface particles ( $81 \pm 8$  to  $85 \pm 9\%$ ; **Table 3**) which dominated the isotopic trends (**Figure 3**), the observed minor differences were consistent with the hypothesis of the capture of resuspension events. Generally the lower trap was significantly depleted in  $^{14}\text{C}$  relative to the upper trap (difference of  $\sim 24\%$ ), indicating that resuspension from the seafloor influenced the bottom trap. Consistent with this observation, sinking matter collected in traps 2–4 m above the seafloor had  $\Delta^{14}\text{C}$  values of  $-71 \pm 39\%$  and  $-105 \pm 32\%$  before and after the spill (Prouty et al., 2016). These values are depleted relative to our values, as were their  $\delta^{34}\text{S}$  values ( $8.1 \pm 1.6\%$  in 2008–2009 to  $0.5 \pm 2.4\%$ ), indicating that carbon age and  $\delta^{34}\text{S}$  of settling matter increase and decrease, respectively, closer to the seafloor, possibly as a result of more sediment resuspension. On three occasions, however, the upper trap was more depleted, consistent with interpretation of periodic resuspension and lateral transport from the slope (see also Diercks et al., 2018).

### 4.4. A natural MOSSFA event?

Giering et al. (2018) postulated that the flux data captured a natural MOSSFA event at the Seep site, during which the presence of crude oil in the trap was revealed by various hydrocarbon indicators. Around three months later (September 2012–January 2013), the  $\Delta^{14}\text{C}$  signal became unusually depleted, despite no obvious presence of hydrocarbon indicators (**Figures 2 and 4**). Giering et al. (2018) postulated that this older  $^{14}\text{C}$ -depleted material could have originated from petrocarbon incorporation into the food web: as petrogenic molecules are utilized by microbes, the original chemical structures are altered while the isotopic signal is preserved. The  $\delta^{34}\text{S}$  of the Seep site POC supports this hypothesis of re-worked organic material, as it is marine-like over the period. We explore this hypothesis further here.

The inverse correlation between  $\Delta^{14}\text{C}$  and lithogenic matter flux at the Seep site could also implicate the admixture of either river-derived material or resuspended sediments from the shelf (**Figure 5**). The  $\Delta^{14}\text{C}$  depletion during September 2012 and January 2013 could hence be explained by several scenarios: 1) lithogenic material comes from the river and is strongly coupled to riverine 'old' organic matter; 2) lithogenic material comes from the shelf/nearby slope, perhaps along an isopycnal, and is strongly coupled to shelf-sediment 'old' organic matter; 3) lithogenic material comes from local resuspension below the trap and is strongly coupled to benthic 'old'

organic matter; and 4) lithogenic matter acts as ballast for reworked petrocarbon by microbes which aggregates the lithogenic matter (as postulated by Giering et al., 2018; see also Passow, 2004; Passow and De La Rocha, 2006; De La Rocha et al., 2008).

Arguing against resuspension (scenarios 2 and 3 above) are the lack of benthic indicator species in the traps (Yan et al., 2016) and the observation that the trap at 120 mab at the DWH site (which was deployed at a similar distance to the seafloor, but even closer to the shelf) was not strongly influenced by resuspension (see discussion above). In addition, resuspension events are generally of short-term duration, and thus should not leave a clear signature in the trap that averages over a period of several months (Diercks et al., 2018). Thus, we are inclined towards explaining the trough in the Seep site carbon isotope data as a result of either river-derived material or reworked petrocarbon (i.e., scenarios 1 or 4 above) or both.

According to our source analysis, the fluxes at the Seep site were hardly influenced by riverine terrestrial carbon ( $0 \pm 6\%$  to  $3 \pm 6\%$ ; **Table 3**). This finding is in line with the conclusion that the Seep site was less influenced by the river plume than the DWH site (Giering et al., 2018; Diercks et al., 2018). However, an investigation of the mesoscale circulation suggests that particle fluxes in the northern Gulf of Mexico are strongly influenced by mesoscale eddies and the Loop Current which together can, at times, entrain shelf and riverine waters and advect them to the Seep site (Liu et al., 2018). A simulation of October 2012 strongly suggests that the trap at the Seep site collected particles originating from the shelf and the Atchafalaya River (Liu et al., 2018), supporting scenario 1.

However, if the influence of riverine material is the cause for  $\Delta^{14}\text{C}$  depletion in the trap material, why do we not see  $\Delta^{14}\text{C}$  depletion in the two sites that are much more influenced by riverine sources under "background" conditions: the Reference site and the DWH site after July, 2013 (with 20% and 14% riverine C, respectively; **Table 3**)? If the quantity of the riverine material was a powerful determinant of  $\Delta^{14}\text{C}$  and  $\delta^{13}\text{C}$ , we would expect the Reference site and the DWH site (after July 2013) to be consistently depleted in these indicators relative to the Seep site. Yet, such depletion is not the case (**Table 3**), suggesting that advection of 'old' riverine C (scenario 1) cannot fully explain the trough in  $\Delta^{14}\text{C}$  at the Seep site. We are left with scenario 4, which suggests that the trough in  $\Delta^{14}\text{C}$  is caused by microbially reworked hydrocarbon that is then ballasted by lithogenic matter of riverine origin. This conclusion is consistent with the interpretation advanced by Giering et al. (2018). In summary, we suggest that variations in lithogenic flux are associated with variations in petrocarbon-influenced marine snow at the Seep site. The  $\delta^{34}\text{S}$  values during the trough period were marine-like, that is, only slightly depleted relative to the non-trough period, which is consistent with this explanation. Alternatively, the variation in production of transparent exopolymeric particles (TEP) may cause more (or less) binding and sinking of lithogenic particles which are then delivered to the sediment trap (Passow, 2004; Passow and De La Rocha, 2006).

#### 4.5. Carbon sources of the Gulf's sedimenting particles

The equilibrium value to which the system recovers following the perturbation of the oil spill is the new baseline of the system. Whether or not that baseline reflects the pre-spill baseline is, of course, an open question, as little pre-spill data exists with regard to sinking particulates. In our data, the  $\Delta^{14}\text{C}$  values of the POM sink at the DWH site converge on a "recovered" value for  $\Delta^{14}\text{C}$  of  $-3.2 \pm 31\text{‰}$ , while the  $\delta^{13}\text{C}$  value is  $-21.9 \pm 0.5\text{‰}$ . At the Reference site, the  $\Delta^{14}\text{C}$  of  $\text{POM}_{\text{sink}}$  was  $3.8 \pm 31\text{‰}$  with  $\delta^{13}\text{C}$  of  $-21.9 \pm 0.9\text{‰}$ , and at the Seep site, the non-trough  $\Delta^{14}\text{C}$  value was  $-21.7 \pm 45\text{‰}$  while the  $\delta^{13}\text{C}$  value was  $-22.3 \pm 0.5\text{‰}$ . The Reference site and the DWH site reflect somewhat more modern  $^{14}\text{C}$  values and slightly  $^{13}\text{C}$ -enriched values relative to the non-trough values at the Seep site. Sulfur isotope values at the DWH site went from a post-spill low of  $7.4 \pm 3.1\text{‰}$  towards "recovered" values of  $16.9 \pm 2.0\text{‰}$ . At the Reference site,  $\delta^{34}\text{S}$  averaged  $16.2 \pm 3.1\text{‰}$  and at the Seep site was  $17.8 \pm 2.3\text{‰}$ .

What should one expect the isotopic composition of  $\text{POM}_{\text{sink}}$  to be in the northern Gulf of Mexico under "normal" (no oil spill) conditions, and what is the impact of the implied distribution of POM? There are three main sources of fixed carbon contributing to particulates in the Gulf and ultimately to its sediments: recently fixed marine primary production, river-derived material associated with lithogenic particulates, and organic material derived from seafloor seepage of hydrocarbons. Results from the mixing model calculations (**Table 3**) clearly indicate that the baseline isotopic values of sinking POM in the northern Gulf of Mexico were dominated by inputs from recently photosynthesized marine carbon (>80%). The influence of petrocarbon and riverine carbon appeared more episodically, with the former strongly linked to the oil spill and to natural seepage. Thus, the current equilibrium value at the DWH site has likely returned to the pre-spill conditions, it being reasonable that modern photosynthesis would be the primary, though not the only, input. The calculation indicates that the Seep site particulates were also dominated by marine primary production but contained from 5 to 14% petrocarbon. This increase in petroleum inputs is consistent with the overall (non-trough)  $^{14}\text{C}$ - and  $^{13}\text{C}$ -depleted values observed at the Seep site relative to the other two sites, post spill, and the proximity of the site to upwelling of seep-derived fluids (D'souza et al., 2015). River-derived carbon represented as much as  $34 \pm 15\%$  of carbon inputs to the DWH site during the oil spill and  $14 \pm 7\%$  and  $20 \pm 8\%$  to the DWH site after July 2013 and the Reference site respectively, where the latter presumably represents background conditions.

Other assessments of carbon inputs to deep sea sediments have produced somewhat greater assessments for the contribution of riverine carbon. These assessments were based on sediment samples, however, rather than sinking particulates, and may have resulted in a greater estimation of the terrestrial fraction. Waterson and Canuel (2008) proportioned organic material in Gulf sediments into autochthonous (marine) and terrigenous categories.

They reported that the deep sediments of the slope and canyon are 66–73% autochthonous and 27–34% terrestrial, while shelf sediments are 64% autochthonous and 36% terrestrial. Burdige (2005) synthesized a large amount of data and surmised that terrestrial organic matter makes up  $44 \pm 13\%$  of global continental margin sediments and  $36 \pm 11\%$  of all marine sediments. One should expect that source partitioning based on sediment data would reflect more terrestrial inputs than our sediment trap-derived estimates because of selective preservation on the seafloor of degraded river-derived organic matter as opposed to labile fresh plankton inputs (Mead and Goñi, 2008). Sorting and differential sedimentation that occurs across the nearshore to the offshore is important as well (Bianchi et al., 2002). For example, larger material settles close to shore, while more degraded material is carried to deeper waters (Gordon and Goñi, 2003, 2004). Gordon and Goñi (2003; 2004) reported that terrigenous organic matter accounts for about 65–80% of the organics deposited in nearshore shallow water within the 25-m isobath west of the Mississippi river and offshore of the mouth of the Atchafalaya River. But, across the shelf towards deeper water, primary production increases its relative contribution to the carbon flux (Lohrenz et al., 1999; Wysocki et al., 2006). Vertical fluxes of POC in the Mississippi plume can be high (Redalje et al., 1994). Thus one would expect our offshore sediment traps to capture a mix of degraded riverine material and fresh marine organic matter. Once deposited to the seafloor, selective preservation of the already degraded terrestrial fraction was likely.

#### 5. Conclusion

Focusing on our three main objectives, the sinking particulates in the water column near the DWH site appear to have returned to baseline conditions in 3 years following the oil spill based upon a natural abundance radiocarbon metric, in 1–2 years based on hydrocarbon indicators, and in 1–2 years based on  $\delta^{34}\text{S}$  isotopic composition. Baseline conditions for the isotopic composition of sinking POM in this area of the northern Gulf of Mexico are described by the data from the Reference site and the DWH site after July 2013 (**Table 3**). These are the particles that make up the inputs to the sediments of the northern Gulf. Increased  $^{14}\text{C}$  depletion in background surface sediments relative to these sinking POM values (Chanton et al., 2015) must be due to mixing with deeper, older sediments below. There is evidence for a natural MOSSFA event at the Seep site that involves hydrocarbon inputs, depleted radiocarbon values, and interaction with lithogenic material. The northern Gulf of Mexico is a complex system with continual inputs from primary production, riverine runoff, and (natural) seepage; however, surface marine production is the dominant organic matter (>80%) input to sinking particulates. Our data show that long-term monitoring of isotopic signatures in sinking particles provides detailed information on these complex particle dynamics and sources and allows the evaluation of episodic anthropogenic inputs when they occur.

### Data Accessibility Statements

Data deposition: Data are publicly available through the Gulf of Mexico Research Initiative Information & Data Cooperative (GRIIDC) at <https://data.gulfresearchinitiative.org>, DOI: <https://doi.org/10.7266/N737775J>. Detailed notes for each cup and split can be found in the raw data. (DOI: <https://doi.org/10.7266/N7F47M6M>, DOI: <https://doi.org/10.7266/N79C6VHB>, DOI: <https://doi.org/10.7266/N7XK8CZS>, DOI: <https://doi.org/10.7266/N78W3BQJ>, DOI: <https://doi.org/10.7266/N7H993KF>, DOI: <https://doi.org/10.7266/N7CJ8BVQ>, DOI: <https://doi.org/10.7266/N7416VD0>, DOI: <https://doi.org/10.7266/N7PN93PS>, DOI: <https://doi.org/10.7266/N7JW8BXM>, DOI: <https://doi.org/10.7266/N7CR5RQT>, DOI: <https://doi.org/10.7266/N7VT1QGS>, DOI: <https://doi.org/10.7266/N7BR8QKF> and DOI: <https://doi.org/10.7266/N71C1V8T>).

### Acknowledgements

AMS samples were run at the University of Georgia Center for Applied Isotopic Studies, and the National Oceanographic Center for Accelerator Mass Spectrometry at Woods Hole Oceanographic. We thank Alexander Cherinsky, Ann McNichol, Kathryn Elder, and Mark Roberts. Samples were collected from the RV Pelican and the RV Point Sur and we thank their crews. We thank Burt Wolff and Yang Wang for use of the facilities at the Mag Lab and for keeping that gear humming. We thank the editors, particularly Dr. Jody Deming, and two anonymous reviewers for their assistance with this work.

### Funding informations

This research was made possible by a grant from The Gulf of Mexico Research Initiative through its consortia: Ecosystem Impacts of Oil & Gas Inputs to the Gulf (ECOGIG). This is ECOGIG Contribution # 489.

### Competing interests

The authors have no competing interests to declare.

### Author contributions

- Contributed to conception and design: UP, JPC, VA, ARD
- Contributed to acquisition of data: SB, KR, JS, VA, ARD, UP
- Contributed to analysis and interpretation of data: JPC, SLCG, UP, ARD, KR, SB
- Drafted and revised the article: JPC, SLCG, UP, ARD, KR, SB
- Approved the submitted version for publication: All

### References

- Adhikari, PL, Maiti, K and Overton, EB.** 2015. Vertical fluxes of polycyclic aromatic hydrocarbons in the northern Gulf of Mexico. *Mar Chem* **168**: 60–68. DOI: <https://doi.org/10.1016/j.marchem.2014.11.001>
- Alberty, RA and Reif, AK.** 1988. Standard chemical thermodynamic properties of polycyclic aromatic hydrocarbons and their isomer groups I. Benzene series. *J Phys Chem Ref Data* **17**: 241–253. DOI: <https://doi.org/10.1063/1.555823>
- Bauer, JE, Druffel, ERM, Wolgast, DM and Griffin, S.** 2002. Temporal and regional variability in sources and cycling of DOC and POC in the northwest Atlantic continental shelf and slope. *Deep-Sea Res II* **49**: 4387–4419. DOI: [https://doi.org/10.1016/S0967-0645\(02\)00123-6](https://doi.org/10.1016/S0967-0645(02)00123-6)
- Bidigare, RR, Fluegge, A, Freeman, KH, Hanson, KL, Hayes, JM, et al.** 1997. Consistent fractionation of <sup>13</sup>C in nature and in the laboratory: Growth-rate effects in some haptophyte algae. *Global Biogeochem Cy* **11**: 279–292. DOI: <https://doi.org/10.1029/96GB03939>
- Bosman, SH, Chanton, JP and Rogers, KL.** 2017. Chapter 29, Using stable and radiocarbon analyses as a forensic tool to find evidence of oil in the particulates of the water column and on the seafloor following the 2010 Gulf of Mexico Oil Spill. In: Stout, S and Wang, Z (eds.), *Oil Spill Environmental Forensics Case Studies*, 639–650. Cambridge, MA, USA: Butterworth and Heinemann.
- Bouloubassi, I, Méjanelle, L, Pete, R, Fillaux, J, Lorre, A and Point, V.** 2006. PAH transport by sinking particles in the open Mediterranean Sea: A 1 year sediment trap study. *Mar Poll Bull* **52**(5): 560–571. DOI: <https://doi.org/10.1016/j.marpolbul.2005.10.003>
- Brooks, GR, Larson, RA, Schwing, PT, Romero, I, Moore, C, et al.** 2015. Sedimentation pulse in the NE Gulf of Mexico following the 2010 DWH blowout. *PLOS One* **10**(7): e0132341. DOI: <https://doi.org/10.1371/journal.pone.0132341>
- Burdige, DJ.** 2005. Burial of terrestrial organic matter in marine sediments: a re-assessment. *Global Biogeochem Cy* **19**: GB4011. DOI: <https://doi.org/10.1029/2004GB002368>
- Burkhardt, S, Riebesell, U and Zondervan, I.** 1999. Stable carbon isotope fractionation by marine phytoplankton in response to day length, growth rate, and CO<sub>2</sub> availability. *Mar Ecol Prog Ser* **184**: 31–41. DOI: <https://doi.org/10.3354/meps184031>
- Camilli, R, Reddy, CM, Yoerger, DR, Van Mooy, BAS, Jakuba, MV, et al.** 2010. Tracking hydrocarbon plume transport and biodegradation at Deepwater Horizon. *Science* **330**: 201–204. DOI: <https://doi.org/10.1126/science.1195223>
- Chanton, JP, Cherrier, J, Wilson, RM, Sarkodee-Adoo, J, Boseman, S, et al.** 2012. Radiocarbon evidence that carbon from the Deepwater Horizon spill entered the planktonic food web of the Gulf of Mexico. *Environ Res Lett* **7**. DOI: <https://doi.org/10.1088/1748-9326/7/4/045303>
- Chanton, JP and Lewis, FG.** 2002. Examination of coupling between primary and secondary production in a river-dominated estuary: Apalachicola Bay, Florida, USA. *Limnol Oceanogr* **47**: 683–697. DOI: <https://doi.org/10.4319/lo.2002.47.3.0683>

- Chanton, JP, Martens, CS and Goldhaber, MB.** 1987. Biogeochemical cycling in an organic-rich coastal marine basin. 8. A sulfur isotopic budget balanced by differential diffusion across the sediment-water interface. *Geochim Cosmochim Acta* **51**(5): 1201–1208. DOI: [https://doi.org/10.1016/0016-7037\(87\)90212-2](https://doi.org/10.1016/0016-7037(87)90212-2)
- Chanton, JP, Zhao, T, Rosenheim, BE, Joye, S, Bosman, S,** et al. 2015. Using natural abundance radiocarbon to trace the flux of petrocarbon to the seafloor following the Deepwater Horizon oil spill. *Environ Sci Technol* **49**: 847–854. DOI: <https://doi.org/10.1021/es5046524>
- Cherrier, J, Sarkodee-Adoo, J, Guilderson, TP and Chanton, JP.** 2014. Fossil carbon in particulate organic matter in the Gulf of Mexico following the Deep Water Horizon event. *Environ Sci Technol Lett* **1**: 108–112. DOI: <https://doi.org/10.1021/ez400149c>
- Choi, Y and Wang, Y.** 2004. Dynamics of carbon sequestration in a coastal wetland using radiocarbon measurements. *Global Biogeochem Cy* **18**(4): GB4016. DOI: <https://doi.org/10.1029/2004GB002261>
- Crespo-Medina, M, Meile, CD, Hunter, KS, Diercks, A-R, Asper, VL,** et al. 2014. The rise and fall of methanotrophy following a deepwater oil-well blowout. *Nat Geosci* **7**: 423–427. DOI: <https://doi.org/10.1038/ngeo2156>
- Daly, KL, Passow, U, Chanton, J and Hollander, D.** 2016. Assessing the impacts of oil-associated marine snow formation and sedimentation during and after the Deepwater Horizon oil spill. *Anthropocene* **13**: 18–33. DOI: <https://doi.org/10.1016/j.ancene.2016.01.006>
- De La Rocha, CL, Nowald, N and Passow, U.** 2008. Interactions between diatom aggregates, minerals, particulate organic carbon, and dissolved organic matter: Further implications for the ballast hypothesis. *Global Biogeochem Cy* **22**(4): GB4005. DOI: <https://doi.org/10.1029/2007GB003156>
- Diercks, A-R and Asper, VL.** 1997. In situ settling speeds of marine snow aggregates below the mixed layer: Black Sea and Gulf of Mexico. *Deep Sea Res Part I* **44**(3): 385–398. DOI: [https://doi.org/10.1016/S0967-0637\(96\)00104-5](https://doi.org/10.1016/S0967-0637(96)00104-5)
- Diercks, A-R, Dike, C, Asper, VL, DiMarco, SF, Chanton, JP,** et al. 2018. Resuspension scales in the northern Gulf of Mexico. *Elem Sci Anth* (in press). DOI: <https://doi.org/10.1525/elementa.285>
- Diercks, A-R, Highsmith, RC, Asper, VL, Joung, D, Zhou, Z,** et al. 2010. Characterization of subsurface polycyclic aromatic hydrocarbons at the Deepwater Horizon site. *Geophys Res Lett* **37**(20): L20602. DOI: <https://doi.org/10.1029/2010GL045046>
- D'souza, NA, Subramaniam, A, Juhl, AR, Hafez, M, Chekalyuk, A,** et al. 2016. Elevated surface chlorophyll associated with natural oil seeps in the Gulf of Mexico. *Nat Geosci* **9**: 215–218. DOI: <https://doi.org/10.1038/ngeo2631>
- Fisher, CR, Hsing, P-Y, Kaiser, CL, Yoerger, DR, Roberts, HH,** et al. 2014. Footprint of Deepwater Horizon blowout impact to deep-water coral communities. *P Natl Acad Sci USA* **111**(32): 11744–11749. DOI: <https://doi.org/10.1073/pnas.1403492111>
- Garcia-Pineda, O, MacDonald, I, Hu, C, Svejksky, J, Hess, M,** et al. 2013. Detection of floating oil anomalies from the Deepwater Horizon oil spill with synthetic aperture radar. *Oceanography* **26**: 124–137. DOI: <https://doi.org/10.5670/oceanog.2013.38>
- Giering, SLC, Yan, B, Sweet, J, Asper, V, Diercks, A,** et al. 2018. The ecosystem baseline for particle flux in the Northern Gulf of Mexico. *Elem Sci Anth*. DOI: <https://doi.org/10.1525/elementa.264>
- Gordon, ES and Goñi, MA.** 2003. Sources and distribution of terrigenous organic matter delivered by the Atchafalaya River to sediments in the northern Gulf of Mexico. *Geochim Cosmochim Acta* **67**: 2359–2375. DOI: [https://doi.org/10.1016/S0016-7037\(02\)01412-6](https://doi.org/10.1016/S0016-7037(02)01412-6)
- Gordon, ES and Goñi, MA.** 2004. Controls on the distribution and accumulation of terrigenous organic matter in sediments from the Mississippi and Atchafalaya River margin. *Mar Chem* **92**: 331–352. DOI: <https://doi.org/10.1016/j.marchem.2004.06.035>
- Graham, WM, Condon, RH, Carmichael, RH, D'Ambra, I, Patterson, HK,** et al. 2010. Oil carbon entered the coastal planktonic food web during the Deepwater Horizon oil spill. *Environ Res Lett* **5**: 6.
- Griffiths, SK.** 2012. Oil release from Macondo well MC252 following the Deepwater Horizon accident. *Environ Sci Technol* **46**: 5616–5622. DOI: <https://doi.org/10.1021/es204569t>
- Hovland, M.** 2002. On the self-sealing nature of marine seeps. *Cont Shelf Res* **22**: 2387–2394. DOI: [https://doi.org/10.1016/S0278-4343\(02\)00063-8](https://doi.org/10.1016/S0278-4343(02)00063-8)
- Joye, SB, MacDonald, IR, Leifer, I and Asper, V.** 2011. Magnitude and oxidation potential of hydrocarbon gases released from the BP oil well blowout. *Nat Geosci* **4**: 160–165. DOI: <https://doi.org/10.1038/ngeo1067>
- Killick, R, Beaulieu, C and Taylor, S.** 2016. EnvCpt: Detection of Structural Changes in Climate and Environment Time Series. R package version 0.1.1. <https://CRAN.R-project.org/package=EnvCpt>.
- Lapham, LL, Chanton, JP, Martens, CS, Higley, PD, Jannasch, HW,** et al. 2008a. Measuring temporal variability in pore-fluid chemistry to assess gas hydrate stability: development of a continuous pore-fluid array. *Environ Sci Technol* **42**: 7368–7373. DOI: <https://doi.org/10.1021/es801195m>
- Lapham, LL, Chanton, JP, Martens, CS, Sleeper, K and Woolsey, JR.** 2008b. Microbial activity in surficial sediments overlying acoustic wipe-out zones at a Gulf of Mexico cold seep. *Geochem Geophys* **9**: Q06001. DOI: <https://doi.org/10.1029/2008GC001944>
- Laws, EA, Popp, BN, Bidigare, RR, Kennicutt, MC and Macko, SA.** 1995. Dependence of phytoplankton carbon isotopic composition on growth rate and

- [CO<sub>2</sub>]<sub>aq</sub>: Theoretical considerations and experimental results. *Geochim Cosmochim Acta* **59**(6): 1131–1138. DOI: [https://doi.org/10.1016/0016-7037\(95\)00030-4](https://doi.org/10.1016/0016-7037(95)00030-4)
- Lehr, W, Bristol, S and Possolo, A.** 2010. Federal Interagency Solutions Group, Oil budget calculator science and engineering team. Oil Budget Calculator. Technical document. Available at: [http://www.restorethegulf.gov/sites/default/files/documents/pdf/OilBudgetCalc\\_Full\\_HQ-Print\\_111110.pdf](http://www.restorethegulf.gov/sites/default/files/documents/pdf/OilBudgetCalc_Full_HQ-Print_111110.pdf).
- Liu, G, Bracco, A and Passow, U.** 2018. Mesoscale and submesoscale circulation influences sinking particles in the northern Gulf of Mexico. *Elem Sci Anth* (in press). DOI: <https://doi.org/10.1525/elementa.292>
- Lohrenz, SE, Fahnenstiel, GL, Redalje, DG, Lang, GA, Chen, X and Dagg, MJ.** 1999. Variations in primary production of northern Gulf of Mexico continental shelf waters linked to nutrient inputs from the Mississippi River. *Mar Ecol Prog Ser* **155**: 45–54. DOI: <https://doi.org/10.3354/meps155045>
- MacDonald, I, Guinasso, NL, Jr., Acchleson, SG, Amos, JF, Duckworth, R, et al.** 1993. Natural oil slicks in the Gulf of Mexico visible from space. *J Geophys Res* **98**: 16351–16364. DOI: <https://doi.org/10.1029/93JC01289>
- MacDonald, IR, Garcia-Pineda, O, Beet, A, Daneshgar Asi, S, Feng, L, et al.** 2015. Natural and unnatural oil slicks in the Gulf of Mexico. *J Geophys Res: Oceans* **120**(12): 8364–8380. DOI: <https://doi.org/10.1002/2015JC011062>
- MacDonald, IR, Leifer, I, Sassen, R, Stine, P, Mitchell, R, et al.** 2002. Transfer of hydrocarbons from natural seeps to the water column and atmosphere. *Geofluids* **2**(2): 95–107. DOI: <https://doi.org/10.1046/j.1468-8123.2002.00023.x>
- McNichol, AP and Aluwihare, LI.** 2007. The power of radiocarbon in biogeochemical studies of the marine carbon cycle: Insights from studies of dissolved and particulate organic carbon (DOC and POC). *Chem Rev* **107**(2): 443–466. DOI: <https://doi.org/10.1021/cr050374g>
- McNutt, MK, Camilli, R, Crone, TJ, Guthrie, GD, Hsieh, PA, et al.** 2012. Review of flow rate estimates of the Deepwater Horizon oil spill. *P Natl Acad Sci USA* **109**: 20260–20267. DOI: <https://doi.org/10.1073/pnas.1112139108>
- Muschenheim, DK and Lee, K.** 2002. Removal of oil from the sea surface through particulate interactions: review and prospectus. *Spill Sci Technol Bull* **8**: 9–18. DOI: [https://doi.org/10.1016/S1353-2561\(02\)00129-9](https://doi.org/10.1016/S1353-2561(02)00129-9)
- Passow, U.** 2004. Switching perspectives: Do mineral fluxes determine particulate organic carbon fluxes or vice versa? *Geochem Geophys* **5**(4): Q04002. DOI: <https://doi.org/10.1029/2003GC000670>
- Passow, U and De La Rocha, CL.** 2006. Accumulation of mineral ballast on organic aggregates. *Global Biogeochem Cy* **20**(1): GB1013. DOI: <https://doi.org/10.1029/2005GB002579>
- Passow, U and Hetland, RD.** 2016. What happened to all of the oil? *Oceanography* **29**(3): 88–95. DOI: <https://doi.org/10.5670/oceanog.2016.73>
- Passow, U and Ziervogel, K.** 2016. Marine snow sedimented oil released during the Deepwater Horizon spill. *Oceanography* **29**(3): 118–125. DOI: <https://doi.org/10.5670/oceanog.2016.76>
- Passow, U, Ziervogel, K, Asper, V and Diercks, A.** 2012. Marine snow formation in the aftermath of the Deepwater Horizon oil spill in the Gulf of Mexico. *Environ Res Lett* **7**(3): 11. DOI: <https://doi.org/10.1088/1748-9326/7/3/035301>
- Prouty, NG, Campbell, PL, Mienis, F, Duineveld, G, Demopoulos, AWJ, et al.** 2016. Impact of Deepwater Horizon spill on food supply to deep-sea benthos communities. *Estuar Coast Shelf Sci* **169**: 248–264. DOI: <https://doi.org/10.1016/j.ecss.2015.11.008>
- Rau, GH, Riebesell, U and Wolf-Gladrow, D.** 1997. CO<sub>2</sub>-dependent photosynthetic <sup>13</sup>C fractionation in the ocean: A model versus measurements. *Global Biogeochem Cy* **11**(2): 267–278. DOI: <https://doi.org/10.1029/97GB00328>
- Redalje, DG and Fahnenstiel, GL.** 1994. The relationship between primary production and the vertical export of particulate organic matter in a river-impacted coastal ecosystem. *Estuaries* **17**: 829–838. DOI: <https://doi.org/10.2307/1352751>
- Reddy, CM, Pearson, A, Xu, L, McNichol, A, Benner, BA, Jr., et al.** 2002. Radiocarbon as a tool to apportion the sources of polycyclic aromatic hydrocarbons and black carbon in environmental samples. *Environ Sci Technol* **36**: 1774–1782. DOI: <https://doi.org/10.1021/es011343f>
- Rees, CE, Jenkins, WJ and Monster, J.** 1978. The sulphur isotopic composition of ocean water sulphate. *Geochim Cosmochim Acta* **42**(4): 377–381. DOI: [https://doi.org/10.1016/0016-7037\(78\)90268-5](https://doi.org/10.1016/0016-7037(78)90268-5)
- Roberts, HH and Carney, RS.** 1997. Evidence of episodic fluid, gas, and sediment venting on the northern Gulf of Mexico continental slope. *Econ Geol* **92**(7–8): 863–879. DOI: <https://doi.org/10.2113/gsecongeo.92.7-8.863>
- Romero, IC, Toro-Farmer, G, Diercks, A-R, Schwing, P, Muller-Karger, F, et al.** 2017. Large-scale deposition of weathered oil in the Gulf of Mexico following a deep-water oil spill. *Environ Pollut* **228**: 179–189. DOI: <https://doi.org/10.1016/j.envpol.2017.05.019>
- Rosenheim, BE, Pendergraft, MA, Flowers, GC, Carney, R, Sericano, J, et al.** 2016. Employing extant stable carbon isotope data in Gulf of Mexico sedimentary organic matter for oil spill studies. *Deep Sea Res II* **129**: 249–258. DOI: <https://doi.org/10.1016/j.dsr2.2014.03.020>
- Rosenheim, BE, Roe, KM, Roberts, BJ, Kolker, AS, Allison, MA, et al.** 2013. River discharge influences on particulate organic carbon age structure in the Mississippi/Atchafalaya River System. *Global Biogeochem Cy* **27**: 154–166. DOI: <https://doi.org/10.1002/gbc.20018>

- Ruddy, BM, Huettel, M, Kostka, JE, Lobodin, VV, Bythell, BJ**, et al. 2014. Targeted petroleomics: Analytical investigation of Macondo well oil oxidation products from Pensacola Beach. *Energ Fuel* **28**(6): 4043–4050. DOI: <https://doi.org/10.1021/ef500427n>
- Schwing, PT, Brooks, GR, Larson, RA, Holmes, CW, O'Malley, BJ**, et al. 2017. Constraining the spatial extent of marine oil snow sedimentation and flocculent accumulation (MOSSFA) following the Deepwater Horizon event using an excess  $^{210}\text{Pb}$  flux approach. *Environ Sci Technol* **51**(11): 5962–5968. DOI: <https://doi.org/10.1021/acs.est.7b00450>
- Solomon, EA, Kastner, M, MacDonald, IR and Leifer, I**. 2009. Considerable methane fluxes to the atmosphere from hydrocarbon seeps in the Gulf of Mexico. *Nat Geosci* **2**(8): 561–565. DOI: <https://doi.org/10.1038/ngeo574>
- Stout, SA and German, CR**. 2015. Characterization and flux of marine oil snow into the Viosca Knoll (Lophelia Reef) area due to the Deepwater Horizon oil spill. US Department of the Interior, Deepwater Horizon Response and Restoration, Administrative Record. Available at: <https://www.fws.gov/doid-data/dwh-ar-documents/946/DWH-AR0039084.pdf>.
- Stout, SA and Passow, U**. 2015. Character and sedimentation rate of “lingering” Macondo oil in the deep sea up to one year after the Deepwater Horizon oil spill. US Department of Interior, Deepwater Horizon Response and Restoration, Administrative Record: **34**. <https://pub-dwhdatadiver.orr.noaa.gov/dwh-ar-documents/946/DWH-AR0038895.pdf>.
- Stout, SA, Rouhani, S, Liu, B, Oehrig, J, Ricker, RW**, et al. 2017. Assessing the footprint and volume of oil deposited in deep-sea sediments following the Deepwater Horizon oil spill. *Mar Pollut Bull* **114**(1): 327–342. DOI: <https://doi.org/10.1016/j.marpolbul.2016.09.046>
- Stuiver, M and Polach, HA**. 1977. Reporting Of  $^{14}\text{C}$  Data. *Radiocarbon* **19**: 355–263. DOI: <https://doi.org/10.1017/S0033822200003672>
- Valentine, DL, Fisher, GB, Bagby, SC, Nelson, RK, Reddy, CM**, et al. 2014. Fallout plume of submerged oil from Deepwater Horizon. *P Natl Acad Sci USA* **111**(45): 15906–15911. DOI: <https://doi.org/10.1073/pnas.1414873111>
- Valentine, DL, Kessler, JD, Redmond, MC, Mendes, SD, Heintz, MB**, et al. 2010. Propane respiration jump-starts microbial response to a deep oil spill. *Science* **330**: 208–211. DOI: <https://doi.org/10.1126/science.1196830>
- Vogel, JS, Southon, JR, Nelson, DE and Brown, TA**. 1984. Performance of catalytically condensed carbon for use in Accelerator Mass-Spectrometry. *Nuclear Instruments and Methods in Physics Research Section B Beam Interactions with Materials and Atoms* **5**: 289–293. DOI: [https://doi.org/10.1016/0168-583X\(84\)90529-9](https://doi.org/10.1016/0168-583X(84)90529-9)
- Waterson, EJ and Canuel, EA**. 2008. Sources of sedimentary organic matter in the Mississippi River and adjacent Gulf of Mexico as revealed by lipid biomarker and  $\delta^{13}\text{C}_{\text{TOC}}$  analyses. *Org Geochem* **39**: 422–439. DOI: <https://doi.org/10.1016/j.orggeochem.2008.01.011>
- White, HK, Reddy, CM and Eglinton, TI**. 2005. Isotopic constraints on the fate of petroleum residues sequestered in salt marsh sediments. *Environ Sci Technol* **8**(15): 2545–2551. DOI: <https://doi.org/10.1021/es048675f>
- White, HK, Reddy, CM and Eglinton, TI**. 2008. Radiocarbon-based assessment of fossil fuel-derived contaminant associations in sediments. *Environ Sci Technol* **42**(15): 5428–5434. DOI: <https://doi.org/10.1021/es800478x>
- Wilson, RM, Cherrier, J, Sarkodee-Adoo, J, Bosman, S, Mickle, A**, et al. 2016. Tracing the intrusion of fossil carbon into coastal Louisiana macrofauna using natural  $^{14}\text{C}$  and  $^{13}\text{C}$  abundances. *Deep-Sea Res II* **129**: 89–95. DOI: <https://doi.org/10.1016/j.dsr2.2015.05.014>
- Wysocki, LA, Bianchi, TS, Powell, RT and Reuss, N**. 2006. Spatial variability in the coupling of organic carbon, nutrients, and phytoplankton pigments in surface waters and sediments of the Mississippi river plume. *Estuar Coast Shelf Sci* **69**: 47–63. DOI: <https://doi.org/10.1016/j.ecss.2006.03.022>
- Yan, B, Passow, U, Chanton, JP, Nöthig, E-M, Asper, V**, et al. 2016. Sustained deposition of contaminants from the Deepwater Horizon spill. *P Natl Acad Sci* **113**: E3332–E3340. DOI: <https://doi.org/10.1073/pnas.1513156113>

**How to cite this article:** Chanton, JP, Giering, SLC, Bosman, SH, Rogers, KL, Sweet, J, Asper, VL, Diercks, AR and Passow, U. 2018. Isotopic composition of sinking particles: Oil effects, recovery and baselines in the Gulf of Mexico, 2010–2015. *Elem Sci Anth*, 6: 43. DOI: <https://doi.org/10.1525/elementa.298>

**Domain Editor-in-Chief:** Jody W. Deming, Department of Biological Oceanography, University of Washington, US

**Associate Editor:** Lisa A. Miller, Institute of Ocean Sciences, Fisheries and Oceans Canada, CA

**Knowledge Domain:** Ocean Science

**Part of an *Elementa* Feature:** Impacts of Natural Versus Anthropogenic Oil Inputs on the Gulf of Mexico Ecosystem

**Submitted:** 10 October 2017    **Accepted:** 12 May 2018    **Published:** 30 May 2018

**Copyright:** © 2018 The Author(s). This is an open-access article distributed under the terms of the Creative Commons Attribution 4.0 International License (CC-BY 4.0), which permits unrestricted use, distribution, and reproduction in any medium, provided the original author and source are credited. See <http://creativecommons.org/licenses/by/4.0/>.



*Elem Sci Anth* is a peer-reviewed open access journal published by University of California Press.

OPEN ACCESS 